Biomolecular Feedback Systems

Domitilla Del Vecchio
MIT

Richard M. Murray
Caltech

Version 1.0a, January 19, 2014

This is the electronic edition of *Biomolecular Feedback Systems* and is available from http://www.cds.caltech.edu/~murray/BFS. Hardcover editions may be purchased from Princeton Univeristy Press, `http://press.princeton.edu/titles/10285.html`.

Chapter 6
Interconnecting Components

In Chapter 2 and Chapter 5 we studied the behavior of simple biomolecular modules, such as oscillators, toggles, self repressing circuits, signal transduction and amplification systems, based on reduced order models. One natural step forward is to create larger and more complex systems by composing these modules together. In this chapter, we illustrate problems that need to be overcome when interconnecting components and propose a number of engineering solutions based on the feedback principles introduced in Chapter 3. Specifically, we explain how loading effects arise at the interconnection between modules, which change the expected circuit behavior. These loading problems appear in several other engineering domains, including electrical, mechanical, and hydraulic systems, and have been largely addressed by the respective engineering communities. In this chapter, we explain how similar engineering solutions can be employed in biomolecular systems to defeat loading effects and guarantee "modular" interconnection of circuits. In Chapter 7, we further study loading of the cellular environment by synthetic circuits employing the same framework developed in this chapter.

6.1 Input/Output Modeling and the Modularity Assumption

The input/output modeling introduced in Chapter 1 and further developed in Chapter 3 has been employed so far to describe the behavior of various modules and subsystems. This input/output description of a system allows to connect systems together by setting the input u_2 of a downstream system equal to the output y_1 of

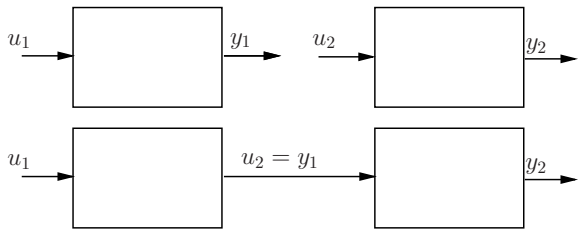

Figure 6.1: In the input/output modeling framework, systems are interconnected by statically assigning the value of the output of the upstream system to the input of the downstream system.

the upstream system (Figure 6.1) and has been extensively used in the previous chapters.

Each node of a gene circuit, such as those in Figure 5.1 of the previous chapter, has been modeled as an input/output system taking the concentrations of transcription factors as input and giving, through the processes of transcription and translation, the concentration of another transcription factor as an output. For example, node C in the repressilator has been modeled as a second order system that takes the concentration of transcription factor B as an input through the Hill function and gives transcription factor C as an output. This is of course not the only possible choice for decomposing the system. We could in fact let the mRNA or the RNA polymerase flowing along the DNA, called PoPS (polymerase per second) [28], play the role of input and output signals. Similarly, a signal transduction network is usually composed of protein covalent modification modules, which take a modifying enzyme (a kinase in the case of phosphorylation) as an input and gives the modified protein as an output.

This input/output modeling framework is extremely useful because it allows us to predict the behavior of an interconnected system from the behavior of the isolated modules. For example, the location and number of equilibria in the toggle switch of Section 5.3 were predicted by intersecting the steady state input/output characteristics, determined by the Hill functions, of the isolated modules A and B. Similarly, the number of equilibria in the repressilator of Section 5.4 was predicted by modularly composing the input/output steady state characteristics, again determined by the Hill functions, of the three modules composing the circuit. Finally, criteria for the existence of a limit cycle in the activator-repressor clock of Section 5.5 were based on comparing the speed of the activator module's dynamics to that of the repressor module's dynamics.

For this input/output interconnection framework to reliably predict the behavior of connected modules, it is necessary that the input/output (dynamic) behavior of a system does not change upon interconnection to another system. We refer to the property by which a system input/output behavior does not change upon interconnection as *modularity*. All the designs and models described in the previous chapter assume that the modularity property holds. In this chapter, we question this assumption and investigate when modularity holds in gene and in signal transduction circuits. Further, we illustrate design methods, based on the techniques of Chapter 3, to create functionally modular systems.

6.2 Introduction to Retroactivity

The modularity assumption implies that when two modules are connected together, their behavior does not change because of the interconnection. However, a fundamental systems engineering issue that arises when interconnecting subsystems is how the process of transmitting a signal to a "downstream" component affects the

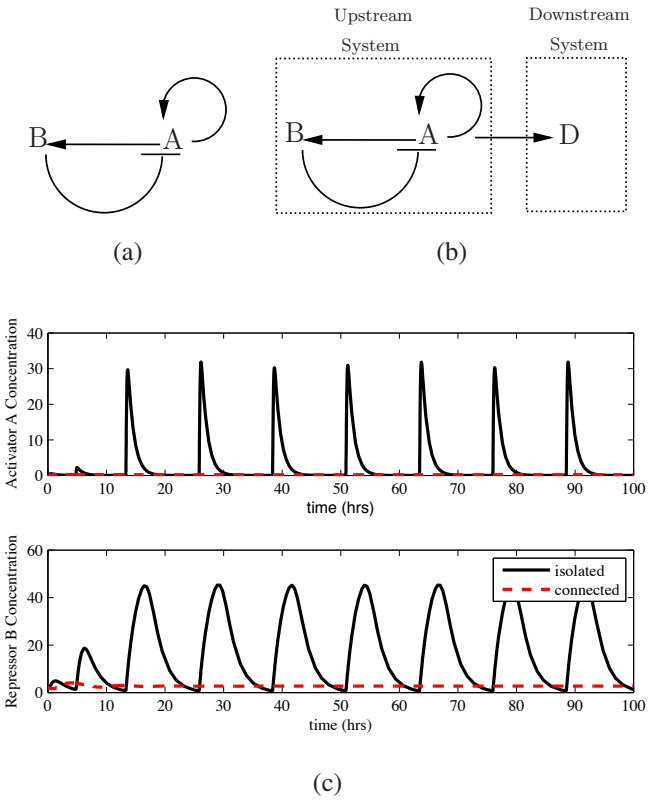

Figure 6.2: Interconnection of an activator-repressor clock to a downstream system. (a) The activator-repressor clock is isolated. (b) The clock is connected to a downstream system. (c) When the clock is connected, perodic behavior of the proteins concentrations is lost and oscillations are quenched. The clock hance fails to transmit the desired periodic stimulation to the downstream system. In all simulations, we have chosen the parameters of the clock as in Figure 5.9. For system in (b), we added the reversible binding reaction of A with sites p in the downstream system: $\mathrm{nA} + \mathrm{p} \rightleftharpoons \mathrm{C}$ with conservation law $p_{\mathrm{tot}} = p + C$, with $p_{\mathrm{tot}} = 5\mathrm{nM}$, association rate constant $k_{\mathrm{on}} = 50\ \mathrm{min}^{-1}\ \mathrm{nM}^{-n}$, and dissociation rate constant $k_{\mathrm{off}} = 50\ \mathrm{min}^{-1}$ (see Exercise 6.12).

dynamic state of the upstream sending component. This issue, the effect of "loads" on the output of a system, is well-understood in many engineering fields such as electrical engineering. It has often been pointed out that similar issues may arise for biological systems. These questions are especially delicate in design problems, such as those described in Chapter 5.

For example, consider a biomolecular clock, such as the activator-repressor clock introduced in Section 5.5 and shown in Figure 6.2a. Assume that the activator protein concentration $A(t)$ is now used as a communicating species to synchronize or provide the timing to a downstream system D (Figure 6.2b). From a systems/signals point of view, $A(t)$ becomes an *input* to the downstream system D.

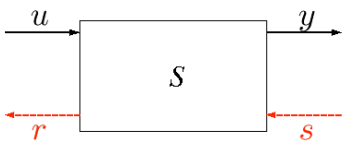

Figure 6.3: A system S input and output signals. The r and s signals denote signals originating by retroactivity upon interconnection [22].

The terms "upstream" and "downstream" reflect the direction in which we think of signals as traveling, *from* the clock *to* the systems being synchronized. However, this is only an idealization because when A is taken as an input by the downstream system it binds to (and unbinds from) the promoter that controls the expression of D. These additional binding/unbinding reactions compete with the biochemical interactions that constitute the upstream clock and may therefore disrupt the operation of the clock itself (Figure 6.2c). We call this back-effect *retroactivity* to extend the notion of impedance or loading to non-electrical systems and in particular to biomolecular systems. This phenomenon, which in principle may be used in an advantageous way by natural systems, can be deleterious when designing synthetic systems.

One possible approach to avoid disrupting the behavior of the clock is to introduce a gene coding for a new protein X, placed under the control of the same promoter as the gene for A, and using the concentration of X, which presumably mirrors that of A, to drive the downstream system. However, this approach still has the problem that the concentration of X may be altered and even disrupted by the addition of downstream systems that drain X, as we shall see in the next section. The net result is that the downstream systems are not properly timed as X does not transmit the desired signal.

To model a system with retroactivity, we add to the input/output modeling framework used so far an additional input, called s, to account for any change that may occur upon interconnection with a downstream system (Figure 6.3). That is, s models the fact that whenever y is taken as an input to a downstream system the value of y may change, because of the physics of the interconnection. This phenomenon is also called in the physics literature "the observer effect", implying that no physical quantity can be measured without being altered by the measurement device. Similarly, we add a signal r as an additional output to model the fact that when a system is connected downstream of another one, it will send a signal upstream that will alter the dynamics of that system. More generally, we define a system S to have internal state x, two types of inputs, and two types of outputs: an input "u", an output "y" (as before), a *retroactivity to the input* "r", and a *retroac-*

tivity to the output "s". We will thus represent a system S by the equations

$$\frac{dx}{dt} = f(x,u,s), \qquad y = h(x,u,s), \qquad r = R(x,u,s), \tag{6.1}$$

where f, g, and R are arbitrary functions and the signals x, u, s, r, and y may be scalars or vectors. In such a formalism, we define the input/output model of the isolated system as the one in equation (6.1) without r in which we have also set $s = 0$.

Let S_i be a system with inputs u_i and s_i and with outputs y_i and r_i. Let S_1 and S_2 be two systems with disjoint sets of internal states. We define the interconnection of an upstream system S_1 with a downstream system S_2 by simply setting $y_1 = u_2$ and $s_1 = r_2$. For interconnecting two systems, we require that the two systems do not have internal states in common.

It is important to note that while retroactivity s is a back action from the downstream system to the upstream one, it is conceptually different from feedback. In fact, retroactivity s is nonzero any time y is transmitted to the downstream system. That is, it is not possible to send signal y to the downstream system without retroactivity s. By contrast, feedback from the downstream system can be removed even when the upstream system sends signal y.

6.3 Retroactivity in Gene Circuits

In the previous section, we have introduced retroactivity as a general concept modeling the fact that when an upstream system is input/output connected to a downstream one, its behavior can change. In this section, we focus on gene circuits and show what form retroactivity takes and what its effects are.

Consider the interconnection of two transcriptional components illustrated in Figure 6.4. A transcriptional component is an input/output system that takes the transcription factor concentration Z as input and gives the transcription factor concentration X as output. The activity of the promoter controlling gene x depends on the amount of Z bound to the promoter. If $Z = Z(t)$, such an activity changes with time and, to simplify notation, we denote it by $k(t)$. We assume here that the mRNA dynamics are at their quasi-steady state. The reader can verify that all the results hold unchanged when the mRNA dynamics are included (see Exercise 6.1). We write the dynamics of X as

$$\frac{dX}{dt} = k(t) - \gamma X, \tag{6.2}$$

in which γ is the decay rate constant of the protein. We refer to equation (6.2) as the *isolated system dynamics*.

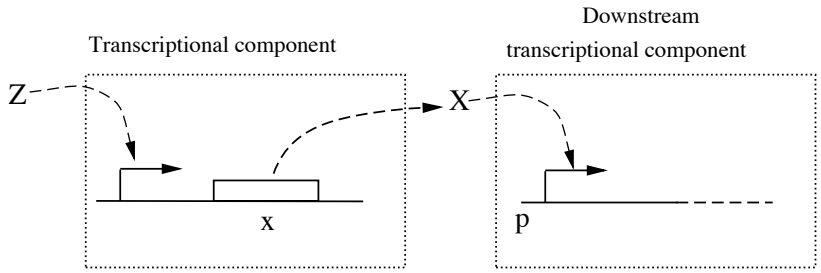

Figure 6.4: A transcriptional component takes as input u protein concentration Z and gives as output y protein concentration X. The downstream transcriptional component takes protein concentration X as its input.

Now, assume that X drives a downstream transcriptional module by binding to a promoter p (Figure 6.4). The reversible binding reaction of X with p is given by

$$\mathrm{X} + \mathrm{p} \underset{k_{\mathrm{off}}}{\overset{k_{\mathrm{on}}}{\rightleftharpoons}} \mathrm{C}$$

in which C is the complex protein-promoter and k_{on} and k_{off} are the association and dissociation rate constants of protein X to promoter site p. Since the promoter is not subject to decay, its total concentration p_{tot} is conserved so that we can write $p + C = p_{\mathrm{tot}}$. Therefore, the new dynamics of X are governed by the equations

$$\frac{dX}{dt} = k(t) - \gamma X + [k_{\mathrm{off}} C - k_{\mathrm{on}}(p_{\mathrm{tot}} - C)X], \qquad \frac{dC}{dt} = -k_{\mathrm{off}} C + k_{\mathrm{on}}(p_{\mathrm{tot}} - C)X. \quad (6.3)$$

We refer to this system as the *connected* system. Comparing the rate of change of X in the connected system to that in the isolated system (6.2), we notice the additional rate of change $[k_{\mathrm{off}} C - k_{\mathrm{on}}(p_{\mathrm{tot}} - C)X]$ of X in the connected system. Hence, we have

$$s = [k_{\mathrm{off}} C - k_{\mathrm{on}}(p_{\mathrm{tot}} - C)X],$$

and $s = 0$ when the system is isolated. We can interpret s as a mass flow between the upstream and the downstream system, similar to a current in electrical circuits.

How large is the effect of retroactivity s on the dynamics of X and what are the biological parameters that affect it? We focus on the retroactivity to the output s as we can analyze the effect of the retroactivity to the input r on the upstream system by simply analyzing the dynamics of Z in the presence of the promoter regulating the expression of gene x.

The effect of retroactivity s on the behavior of X can be very large (Figure 6.5). By looking at Figure 6.5, we notice that the effect of retroactivity is to "slow down" the dynamics of $X(t)$ as the response time to a step input increases and the response

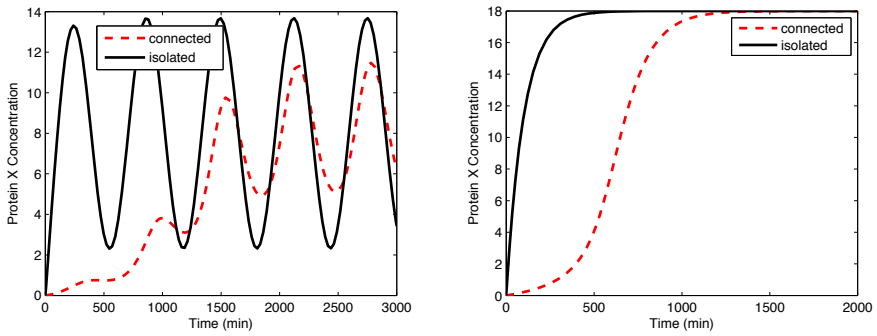

(a) Periodic stimulation (b) Step-like stimulation

Figure 6.5: The effect of retroactivity. The solid line represents $X(t)$ originating by equations (6.2), while the dashed line represents $X(t)$ obtained by equation (6.3). Both transient and permanent behaviors are different. Here, $k(t) = 0.01(8+8sin(\omega t))$ with $\omega = 0.01$ min^{-1} in (a) and $k(t) = 0.18$ in (b). The parameter values are given by $k_{on} = 10$ min^{-1}nM^{-1}, $k_{off} = 10$ min^{-1}, $\gamma = 0.01$ min^{-1}, and $p_{tot} = 100$ nM. The frequency of oscillations is chosen to have a period of about 11 hours in accordance to what is experimentally observed in the synthetic clock of [6].

to a periodic signal appears attenuated and phase-shifted. We will come back to this more precisely in the next section.

These effects are undesirable in a number of situations in which we would like an upstream system to "drive" a downstream one, for example when a biological oscillator has to time a number of downstream processes. If, due to the retroactivity, the output signal of the upstream process becomes too low and/or out of phase with the output signal of the isolated system (as in Figure 6.5), the coordination between the oscillator and the downstream processes will be lost. We next provide a procedure to quantify the effect of retroactivity on the dynamics of the upstream system.

Quantification of the retroactivity to the output

In this section, we provide a general approach to quantify the retroactivity to the output. To do so, we quantify the difference between the dynamics of X in the isolated system (6.2) and the dynamics of X in the connected system (6.3) by establishing conditions on the biological parameters that make the two dynamics close to each other. This is achieved by exploiting the difference of time scales between the protein production and decay processes and binding/unbinding reactions, mathematically described by $k_{off} \gg \gamma$. By virtue of this separation of time scales, we can approximate system (6.3) by a one dimensional system describing the evolution of X on the slow manifold (see Section 3.5).

To this end, note that equation (6.3) is not in standard singular perturbation form: while C is a fast variable, X is neither fast nor slow since its differential equation includes both fast and slow terms. To explicitly model the difference of time scales, we let $z = X + C$ be the total amount of protein X (bound and free) and rewrite system (6.3) in the new variables (z, C). Letting $\epsilon = \gamma/k_{\text{off}}$, $K_d = k_{\text{off}}/k_{\text{on}}$, and $k_{\text{on}} = \gamma/(\epsilon K_{\text{d}})$, system (6.3) can be rewritten as

$$\frac{dz}{dt} = k(t) - \gamma(z - C), \qquad \epsilon\frac{dC}{dt} = -\gamma C + \frac{\gamma}{K_{\text{d}}}(p_{\text{tot}} - C)(z - C), \tag{6.4}$$

in which z is a slow variable. The reader can check that the slow manifold of system (6.4) is locally exponentially stable (see Exercise 6.2).

We can obtain an approximation of the dynamics of X in the limit in which ϵ is very small by setting $\epsilon = 0$. This leads to

$$-\gamma C + \frac{\gamma}{K_{\text{d}}}(p_{\text{tot}} - C)X = 0 \quad \Longrightarrow \quad C = g(X) \text{ with } g(X) = \frac{p_{\text{tot}}X}{X + K_{\text{d}}}.$$

Since $\dot{z} = \dot{X} + \dot{C}$, we have that $\dot{z} = \dot{X} + (dg/dX)\dot{X}$. This along with $\dot{z} = k(t) - \gamma X$ lead to

$$\frac{dX}{dt} = (k(t) - \gamma X)\left(\frac{1}{1 + dg/dX}\right). \tag{6.5}$$

The difference between the dynamics in equation (6.5) (the connected system after a fast transient) and the dynamics in equation (6.2) (the isolated system) is zero when the term $dg(X)/dX$ in equation (6.5) is zero. We thus consider the term $dg(X)/dX$ as a quantification of the retroactivity s after a fast transient in the approximation in which $\epsilon \approx 0$. We can also interpret the term $dg(X)/dX$ as a percentage variation of the dynamics of the connected system with respect to the dynamics of the isolated system at the quasi-steady state. We next determine the physical meaning of such a term by calculating a more useful expression that is a function of key biochemical parameters. Specifically, we have that

$$\frac{dg(X)}{dX} = \frac{p_{\text{tot}}/K_{\text{d}}}{(X/K_{\text{d}} + 1)^2} =: \mathcal{R}(X). \tag{6.6}$$

The retroactivity measure $\mathcal{R}$ is low whenever the ratio $p_{\text{tot}}/K_{\text{d}}$, which can be seen as an effective load, is low. This is the case if the affinity of the binding sites p is small (K_{d} large) or if p_{tot} is low. Also, the retroactivity measure is dependent on X in a nonlinear fashion and it is such that it is maximal when X is the smallest. The expression of $\mathcal{R}(X)$ provides an operative quantification of retroactivity: such an expression can be evaluated once the dissociation constant of X is known, the concentration of the binding sites p_{tot} is known, and X is also measured. From equations (6.5) and (6.6), it follows that the rate of change of X in the connected system is smaller than that in the isolated system, that is, retroactivity slows down

the dynamics of the transcriptional system. This has been also experimentally reported in [49].

Summarizing, the modularity assumption introduced in Section 6.1 holds only when the value of $\mathcal{R}(X)$ is small enough. Thus, the design of a simple circuit can assume modularity if the interconnections among the composing modules can be designed so that the value of $\mathcal{R}(X)$ is low. When designing the system, this can be guaranteed by placing the promoter sites p on low copy number plasmids or even on the chromosome (with copy number equal to 1). High copy number plasmids are expected to lead to non-negligible retroactivity effects on X.

Note however that in the presence of very low affinity and/or very low amount of promoter sites, the amount of complex C will be very low. As a consequence, the amplitude of the transmitted signal to downstream systems may also be very small sot that noise may become a bottleneck. A better approach may be to design insulation devices (as opposed to designing the interconnection for low retroactivity) to buffer systems from possibly large retroactivity as explained later in the chapter.

Effects of retroactivity on the frequency response

In order to explain the amplitude attenuation and phase shift due to retroactivity observed in Figure 6.5, we linearize the system about its equilibrium and determine the effect of retroactivity on the frequency response. To this end, consider the input in the form $k(t) = \bar{k} + A_0 \sin(\omega t)$. Let $X_e = \bar{k}/\gamma$ and $C_e = p_{\text{tot}} X_e/(X_e + K_{\text{d}})$ be the equilibrium values corresponding to $\bar{k}$. The isolated system is already linear, so there is no need to perform linearization and the transfer function from k to X is given by

$$G^i_{Xk}(s) = \frac{1}{s+\gamma}.$$

For the connected system (6.5), let $(\bar{k}, X_e)$ denote the equilibrium, which is the same as for the isolated system, and let $\tilde{k} = k - \bar{k}$ and $x = X - X_e$ denote small perturbations about this equilibrium. Then, the linearization of system (6.5) about $(\bar{k}, X_e)$ is given by

$$\frac{dx}{dt} = (\tilde{k}(t) - \gamma x) \frac{1}{1 + (p_{\text{tot}}/K_{\text{d}})/(X_e/K_{\text{d}} + 1)^2}.$$

Letting $\bar{R} := (p_{\text{tot}}/K_{\text{d}})/(X_e/K_{\text{d}} + 1)^2$, we obtain the transfer function from $\tilde{k}$ to x of the connected system linearization as

$$G^c_{Xk} = \frac{1}{1+\bar{R}} \frac{1}{s + \gamma/(1+\bar{R})}.$$

Hence, we have the following result for the frequency response magnitude and phase shift:

$$M^i(\omega) = \frac{1}{\sqrt{\omega^2 + \gamma^2}}, \qquad \phi^i(\omega) = \tan^{-1}(-\omega/\gamma),$$

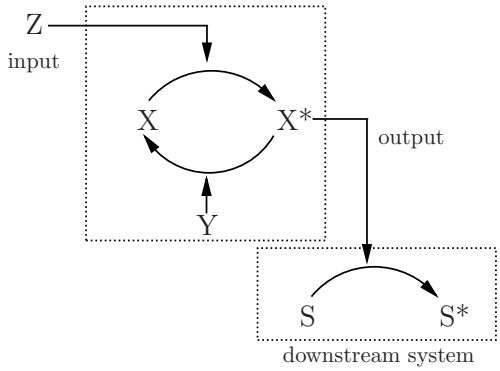

Figure 6.6: Covalent modification cycle with its input, output, and downstream system.

$$M^c(\omega) = \frac{1}{1+\bar{R}} \frac{1}{\sqrt{\omega^2 + \gamma^2/(1+\bar{R})^2}}, \qquad \phi^c(\omega) = \tan^{-1}(-\omega(1+\bar{R})/\gamma),$$

from which one obtains that $M^i(0) = M^c(0)$ and, since $\bar{R} > 0$, the bandwidth of the connected system $\gamma/(1+\bar{R})$ is lower than that of the isolated system γ. As a consequence, we have that $M^i(\omega) > M^c(\omega)$ for all $\omega > 0$. Also, the phase shift of the connected system is larger than that of the isolated system. This explains why the plots of Figure 6.5 show attenuation and a phase shift in the response of the connected system.

When the frequency of the input stimulation $k(t)$ is sufficiently lower than the bandwidth of the connected system $\gamma/(1+\bar{R})$, then the connected and isolated systems will respond similarly. Hence, the effects of retroactivity are tightly related to the time scale properties of the input signals and of the system and mitigation of retroactivity is required only when the frequency range of the signals of interest is larger than the connected system bandwidth $\gamma/(1+\bar{R})$ (see Exercise 6.4).

6.4 Retroactivity in Signaling Systems

Signaling systems are circuits that take external stimuli as inputs and, through a sequence of biomolecular reactions, transform them to signals that control how cells respond to their environment. These systems are usually composed of covalent modification cycles such as phosphorylation, methylation, and urydylilation, and connected in cascade fashion, in which each cycle has multiple downstream targets or substrates (refer to Figure 6.6). An example is the MAPK cascade, which

we have analyzed in Section 2.5. Since covalent modification cycles always have downstream targets, such as DNA binding sites or other substrates, it is particularly important to understand whether and how retroactivity from these downstream systems affects the response of the upstream cycles to input stimulation. In this section, we study this question both for the steady state and transient response of a covalent modification cycle to its input.

Steady state effects of retroactivity

We have seen in Section 2.4 that one important characteristic of signaling systems and, in particular, of covalent modification cycles, is the steady state input/output characteristic curve. We showed in Section 2.4 that when the Michaelis-Menten constants are sufficiently small compared to the amount of total protein, the characteristic curve of the cycle become ultrasensitive, a condition called zero-order ultrasensitivity. When the cycle is connected to its downstream targets, this steady state characteristic curve changes. In order to understand how this happens, we rewrite the reaction rates and the corresponding differential equation model for the covalent modification cycle of Section 2.4, adding the binding of X^* to its downstream target S. Referring to Figure 6.6, we have the following reactions:

$$Z + X \underset{d_1}{\overset{a_1}{\rightleftharpoons}} C_1 \xrightarrow{k_1} X^* + Z, \qquad Y + X^* \underset{d_2}{\overset{a_2}{\rightleftharpoons}} C_2 \xrightarrow{k_2} X + Y,$$

to which we add the binding reaction of X* with its substrate S:

$$X^* + S \underset{k_{\text{off}}}{\overset{k_{\text{on}}}{\rightleftharpoons}} C,$$

in which C is the complex of X* with S. In addition to this, we have the conservation laws $X_{\text{tot}} = X^* + X + C_1 + C_2 + C$, $Z_{\text{tot}} = Z + C_1$, and $Y_{\text{tot}} = Y + C_2$.

The ordinary differential equations governing the system are given by

$$\begin{aligned}
\frac{dC_1}{dt} &= a_1 XZ - (d_1 + k_1)C_1, \\
\frac{dX^*}{dt} &= -a_2 X^* Y + d_2 C_2 + k_1 C_1 - k_{\text{on}} S X^* + k_{\text{off}} C, \\
\frac{dC_2}{dt} &= a_2 X^* Y - (d_2 + k_2)C_2, \\
\frac{dC}{dt} &= k_{\text{on}} X^* S - k_{\text{off}} C.
\end{aligned}$$

The input/output characteristics are found by solving this system for the equilibrium. In particular, by setting $\dot{C}_1 = 0$, $\dot{C}_2 = 0$, using that $Z = Z_{\text{tot}} - C_1$ and that $Y = Y_{\text{tot}} - C_2$, we obtain the familiar expressions for the complexes:

$$C_1 = \frac{Z_{\text{tot}} X}{K_1 + X}, \qquad C_2 = \frac{Y_{\text{tot}} X^*}{K_2 + X^*},$$

with

$$K_1 = \frac{d_1 + k_1}{a_1}, \qquad K_2 = \frac{d_2 + k_2}{a_2}.$$

By setting $\dot{X}^* + \dot{C}_2 + \dot{C} = 0$, we obtain $k_1 C_2 = k_2 C_2$, which leads to

$$V_1 \frac{X}{K_1 + X} = V_2 \frac{X^*}{K_2 + X^*}, \quad V_1 = k_1 Z_{\text{tot}} \quad \text{and} \quad V_2 = k_2 Y_{\text{tot}}. \tag{6.7}$$

By assuming that the substrate X_{tot} is in excess compared to the enzymes, we have that $C_1, C_2 \ll X_{\text{tot}}$ so that $X \approx X_{\text{tot}} - X^* - C$, in which (from setting $dC/dt = 0$) $C = X^* S / K_{\text{d}}$ with $K_{\text{d}} = k_{\text{off}}/k_{\text{on}}$, leading to $X \approx X_{\text{tot}} - X^*(1 + S/K_{\text{d}})$. Calling

$$\lambda = \frac{S}{K_{\text{d}}},$$

equation (6.7) finally leads to

$$y := \frac{V_1}{V_2} = \frac{X^*((K_1/(1+\lambda)) + ((X_{\text{tot}}/(1+\lambda)) - X^*))}{(K_2 + X^*)((X_{\text{tot}}/(1+\lambda)) - X^*)}. \tag{6.8}$$

Here, we can interpret λ as an effective load, which increases with the amount of targets of X^* but also with the affinity of these targets $(1/K_{\text{d}})$.

We are interested in how the shape of the steady state input/output characteristic curve of X^* change as function of y when the effective load λ is changed. As seen in Section 2.4, a way to quantify the sensitivity of the steady state characteristics is to calculate the response coefficient $R = y_{90}/y_{10}$. The maximal value of X^* obtained as $y \to \infty$ is given by $X_{\text{tot}}/(1+\lambda)$. Hence, from equation (6.8), we have that

$$y_{90} = \frac{(\bar{K}_1 + 0.1)0.9}{(\bar{K}_2(1+\lambda) + 0.9)0.1}, \qquad y_{10} = \frac{(\bar{K}_1 + 0.9)0.1}{(\bar{K}_2(1+\lambda) + 0.1)0.9},$$

with

$$\bar{K}_1 := \frac{K_1}{X_{\text{tot}}}, \qquad \bar{K}_2 = \frac{K_2}{X_{\text{tot}}},$$

so that

$$R = 81 \frac{(\bar{K}_1 + 0.1)(\bar{K}_2(1+\lambda) + 0.1}{(\bar{K}_2(1+\lambda) + 0.9)(\bar{K}_1 + 0.9)}.$$

Comparing this expression with the one obtained in equation (2.31) for the isolated covalent modification cycle, we see that the net effect of the downstream target S is that of increasing the Michaelis-Menten constant K_2 by the factor $(1+\lambda)$. Hence, we should expect that with increasing load, the steady state characteristic curve should be more linear-like. This is confirmed by the simulations shown in Figure 6.7 and it was also experimentally demonstrated in signal transduction circuits reconstituted *in vitro* [92].

One can check that R is a monotonically increasing function of λ. In particular, as λ increases, the value of R tends to $81(\bar{K}_1 + 0.1)/(\bar{K}_2 + 0.9)$, which, in turn, tends to 81 for $\bar{K}_1, \bar{K}_2 \to \infty$. When $\lambda = 0$, we recover the results of Section 2.4.

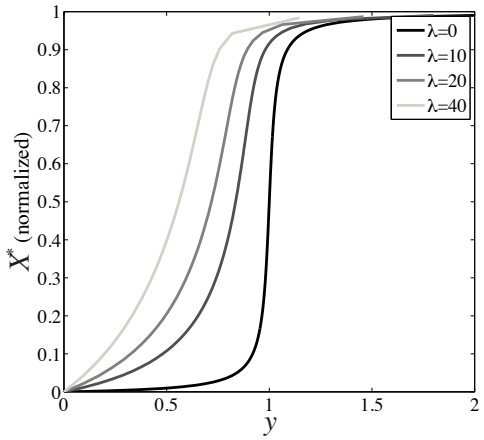

Figure 6.7: Effect of retroactivity on the steady state input/output characteristic curve of a covalent modification cycle. The addition of downstream target sites makes the input/output characteristic curve more linear-like, that is, retroactivity makes a switch-like response into a more graded response. The plot is obtained for $K_1/X_{\text{tot}} = K_2/X_{\text{tot}} = 0.01$ and the value of X^* is normalized to its maximum given by $X_{\text{tot}}/(1+\lambda)$.

Dynamic effects of retroactivity

In order to understand the effects of retroactivity on the temporal response of a covalent modification cycle, we consider changes in Z_{tot} and analyze the temporal response of the cycle to these changes. To perform this analysis more easily, we seek a one dimensional approximation of the X^* dynamics by exploiting time scale separation.

Specifically, we have that $d_i, k_{\text{off}} \gg k_1, k_2$, so we can choose $\epsilon = k_1/k_{\text{off}}$ as a small parameter and $w = X^* + C + C_2$ as a slow variable. By setting $\epsilon = 0$, we obtain $C_1 = Z_{\text{tot}}X/(K_1 + X)$, $C_2 = Y_{\text{tot}}X^*/(K_2 + X^*) =: g(X^*)$, and $C = \lambda X^*$, where Z_{tot} is now a time-varying input signal. Hence, the dynamics of the slow variable w on the slow manifold are given by

$$\frac{dw}{dt} = k_1 \frac{Z_{\text{tot}}(t)X}{K_1 + X} - k_2 Y_{\text{tot}} \frac{X^*}{X^* + K_2}.$$

Using

$$\frac{dw}{dt} = \frac{dX^*}{dt} + \frac{dC}{dt} + \frac{dC_2}{dt}, \quad \frac{dC}{dt} = \lambda \frac{dX^*}{dt}, \quad \frac{dC_2}{dt} = \frac{\partial g}{\partial X^*} \frac{dX^*}{dt},$$

and the conservation law $X = X_{\text{tot}} - X^*(1+\lambda)$, we finally obtain the approximated X^* dynamics as

$$\frac{dX^*}{dt} = \frac{1}{1+\lambda} \left(k_1 \frac{Z_{\text{tot}}(t)(X_{\text{tot}} - X^*(1+\lambda))}{K_1 + (X_{\text{tot}} - X^*(1+\lambda))} - k_2 Y_{\text{tot}} \frac{X^*}{X^* + K_2} \right), \tag{6.9}$$

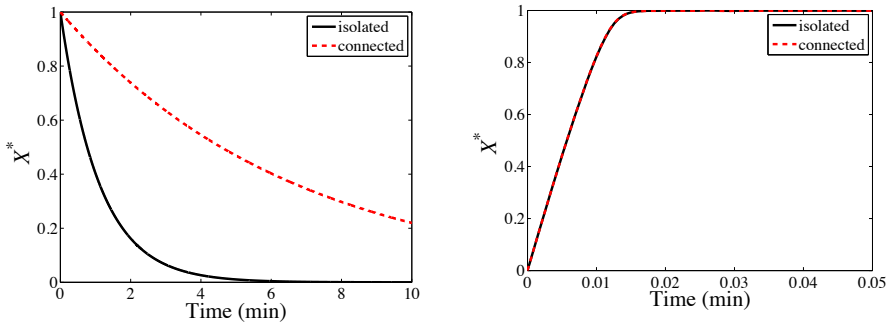

(a) Negative step input (b) Positive step input

Figure 6.8: Effect of retroactivity on the temporal response of a covalent modification cycle. (a) Response to a negative step. The presence of the load makes the response slower. (b) Step response of the cycle in the presence of a positive step. The response time is not affected by the load. Here, $K_1/X_{\text{tot}} = K_2/X_{\text{tot}} = 0.1$, $k_1 = k_2 = 1$ min^{-1}, and $\lambda = 5$. In the plots, the concentration X^* is normalized by X_{tot}.

where we have assumed that $Y_{\text{tot}}/K_2 \ll S/K_{\text{d}}$, so that the effect of the binding dynamics of X* with Y (modeled by $\partial g/\partial X^*$) is negligible with respect to λ. The reader can verify this derivation as an exercise (see Exercise 6.7).

From this expression, we can understand the effect of the load λ on the rise time and decay time in response to large step input stimuli Z_{tot}. For the decay time, we can assume an initial condition $X^*(0) \neq 0$ and $Z_{\text{tot}}(t) = 0$ for all t. In this case, we have that

$$\frac{dX^*}{dt} = -k_2 Y_{\text{tot}} \frac{X^*}{X^* + K_2} \frac{1}{1+\lambda},$$

from which, since $\lambda > 0$, it follows that the transient will be slower than when $\lambda = 0$ and hence that the system will have an increased decay time due to retroactivity. For the rise time, one can assume $Z_{\text{tot}} \approx \infty$ and $X^*(0) = 0$. In this case, at least initially we have that

$$(1+\lambda)\frac{dX^*}{dt} = \left(k_1 \frac{Z_{\text{tot}}(X_{\text{tot}} - X^*(1+\lambda))}{K_1 + (X_{\text{tot}} - X^*(1+\lambda))}\right),$$

which is the same expression for the isolated system in which X^* is scaled by $(1+\lambda)$. So, the rise time is not affected. The response of the cycle to positive and negative steps changes of the input stimulus Z_{tot} are shown in Figure 6.8.

In order to understand how the bandwidth of the system is affected by retroactivity, we consider $Z_{\text{tot}}(t) = \bar{Z} + A_0 \sin(\omega t)$. Let X_e be the equilibrium of X^* corresponding to $\bar{Z}$. Let $z = Z_{\text{tot}} - \bar{Z}$ and $x = X^* - X_e$ denote small perturbations about the equilibrium. The linearization of system (6.9) is given by

$$\frac{dx}{dt} = -a(\lambda)x + b(\lambda)z(t),$$

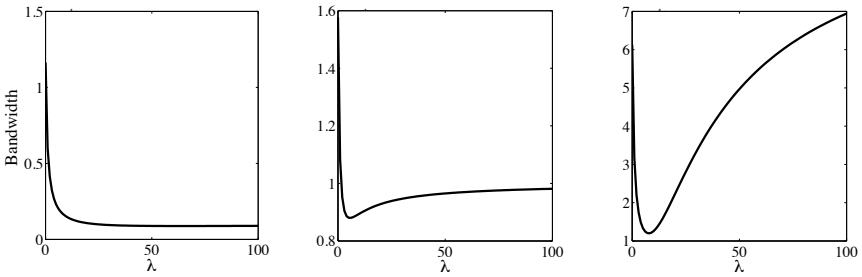

(a) $\bar{K}_1 = \bar{K}_2 = 10$ (b) $\bar{K}_1 = \bar{K}_2 = 1$ (c) $\bar{K}_1 = \bar{K}_2 = 0.1$

Figure 6.9: Behavior of the bandwidth as a function of the effective load λ for different values of the constants $\bar{K}_1, \bar{K}_2$.

in which

$$a(\lambda) = \frac{1}{1+\lambda}\left(k_1\bar{Z}\frac{K_1(1+\lambda)}{(K_1+(X_{\text{tot}}-X_e(1+\lambda)))^2} + k_2 Y_{\text{tot}}\frac{K_2}{(K_2+X_e)^2}\right)$$

and

$$b(\lambda) = \frac{k_1}{1+\lambda}\left(\frac{X_{\text{tot}}-X_e(1+\lambda)}{K_1+(X_{\text{tot}}-X_e(1+\lambda))}\right),$$

so that the bandwidth of the system is given by $\omega_B = a(\lambda)$.

Figure 6.9 shows the behavior of the bandwidth as a function of the load. When the isolated system steady state input/output characteristic curves are linear-like ($K_1, K_2 \gg X_{\text{tot}}$), the bandwidth monotonically decreases with the load. By contrast, when the isolated system static characteristics are ultrasensitive ($K_1, K_2 \ll X_{\text{tot}}$), the bandwidth of the connected system can be larger than that of the isolated system for sufficiently large amounts of loads. In these conditions, one should expect that the response of the connected system becomes faster than that of the isolated system. These theoretical predictions have been experimentally validated in a covalent modification cycle reconstituted *in vitro* [50].

6.5 Insulation Devices: Retroactivity Attenuation

As explained in the previous section, it is not always possible or advantageous to design the downstream system, which we here call module B, such that it applies low retroactivity to the upstream system, here called module A. In fact, module B may already have been designed and optimized for other purposes. A different approach, in analogy to what is performed in electrical circuits, is to design a device to be placed between module A and module B (Figure 6.10) such that the device can

Figure 6.10: An insulation device is placed between an upstream module A and a downstream module B in order to protect these systems from retroactivity. An insulation device should have $r \approx 0$ and the dynamic response of y to u should be practically independent of s.

transmit the output signal of module A to module B even in the presence of large retroactivity s. That is, the output y of the device should follow the behavior of the output of module A independent of a potentially large load applied by module B. This way module B will receive the desired input signal.

Specifically, consider a system S such as the one shown in Figure 6.3. We would like to design such a system such that

(a) the retroactivity r to the input is very small;

(b) the effect of the retroactivity s on the system is very small (retroactivity attenuation);

(c) when $s = 0$, we have that $y \approx Ku$ for some $K > 0$.

Such a system is said to have the *insulation* property and will be called an insulation device. Indeed, such a system does not affect an upstream system because $r \approx 0$ (requirement (a)), it keeps the same output signal $y(t)$ *independently* of any connected downstream system (requirement (b)), and the output is a linear function of the input in the absence of retroactivity to the output (requirement (c)). This requirement rules out trivial cases in which y is saturated to a maximal level for all values of the input, leading to no signal transmission. Of course, other requirements may be important, such as the stability of the device and especially the speed of response.

Equation (6.6) quantifies the effect of retroactivity on the dynamics of X as a function of biochemical parameters. These parameters are the affinity of the binding site $1/K_{\mathrm{d}}$, the total concentration of such binding site p_{tot}, and the level of the signal $X(t)$. Therefore, to reduce retroactivity, we can choose parameters such that $\mathcal{R}(X)$ in equation (6.6) is small. A sufficient condition is to choose K_{d} large (low affinity) and p_{tot} small, for example. Having a small value of p_{tot} and/or low affinity implies that there is a small "flow" of protein X toward its target sites. Thus, we

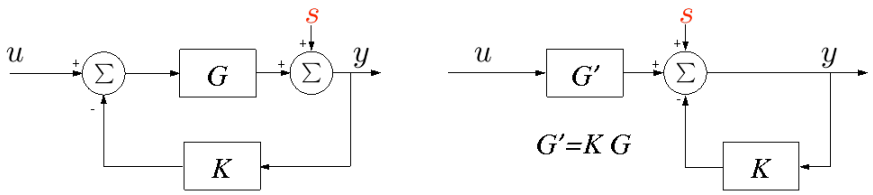

(a) High gain feedback mechanism (b) Alternative representation

Figure 6.11: The block diagram in (a) shows the basic high gain feedback mechanism to attenuate the contribution of disturbance s to the output y. The diagram in (b) shows an alternative representation, which will be employed to design biological insulation devices.

can say that a low retroactivity to the input is obtained when the "input flow" to the system is small. In the next sections, we focus on the retroactivity to the output, that is, on the retroactivity attenuation problem, and illustrate how the problem of designing a device that is robust to s can be formulated as a classical disturbance attenuation problem (Section 3.2). We provide two main design techniques to attenuate retroactivity: the first one is based on the idea of high gain feedback, while the second one uses time-scale separation and leverages the structure of the interconnection.

Attenuation of retroactivity to the output using high gain feedback

The basic mechanism for retroactivity attenuation is based on the concept of disturbance attenuation through high gain feedback presented in Section 3.2. In its simplest form, it can be illustrated by the diagram of Figure 6.11a, in which the retroactivity to the output s plays the same role as an additive disturbance. For large gains G, the effect of the retroactivity s to the output is negligible as the following simple computation shows. The output y is given by

$$y = G(u - Ky) + s,$$

which leads to

$$y = u\frac{G}{1+KG} + \frac{s}{1+KG}.$$

As G grows, y tends to u/K, which is independent of the retroactivity s.

Figure 6.11b illustrates an alternative representation of the diagram depicting high gain feedback. This alternative depiction is particularly useful as it highlights that to attenuate retroactivity we need to (1) amplify the input of the system through a large gain and (2) apply a similarly large negative feedback on the output. The question of how to realize a large input amplification and a similarly large negative feedback on the output through biomolecular interactions is the subject of the

next section. In what follows, we fist illustrate how this strategy also works for a dynamical system of the form of equation (6.5).

Consider the dynamics of the connected transcriptional system given by

$$\frac{dX}{dt} = (k(t) - \gamma X)\left(\frac{1}{1+\mathcal{R}(X)}\right).$$

Assume that we can apply a gain G to the input $k(t)$ and a negative feedback gain G' to X with $G' = KG$. This leads to the new differential equation for the connected system given by

$$\frac{dX}{dt} = \big(Gk(t) - (G' + \gamma)X\big)\,(1 - d(t)), \tag{6.10}$$

in which we have defined $d(t) = \mathcal{R}(X)/(1+\mathcal{R}(X))$. Since $d(t) < 1$, we can verify (see Exercise 6.8) that as G grows $X(t)$ tends to $k(t)/K$ for both the connected system (6.10) and the isolated system

$$\frac{dX}{dt} = Gk(t) - (G' + \gamma)X. \tag{6.11}$$

Specifically, we have the following fact:

Proposition 6.1. *Consider the scalar system $\dot{x} = G(t)(k(t) - Kx)$ with $G(t) \geq G_0 > 0$ and $\dot{k}(t)$ bounded. Then, there are positive constants C_0 and C_1 such that*

$$\left| x(t) - \frac{k(t)}{K} \right| \leq C_0 e^{-G_0 K t} + \frac{C_1}{G_0}.$$

As a consequence, the solutions $X(t)$ of the connected and isolated systems tend to each other as G increases. Hence, the presence of the disturbance $d(t)$ will not significantly affect the time behavior of $X(t)$. It follows that the effect of retroactivity can be arbitrarily attenuated by increasing gains G and G'.

The next questions we address is how we can implement such amplification and feedback gains in a biomolecular system.

Biomolecular realizations of high gain feedback

In this section, we illustrate two possible biomolecular implementations to obtain a large input amplification gain and a similarly large negative feedback on the output. Both implementations realize the negative feedback through enhanced degradation. The first design realizes amplification through transcriptional activation, while the second design uses phosphorylation.

Design 1: Amplification through transcriptional activation

This design is depicted in Figure 6.12. We implement a large amplification of the input signal $Z(t)$ by having Z be a transcription activator for protein X, such that

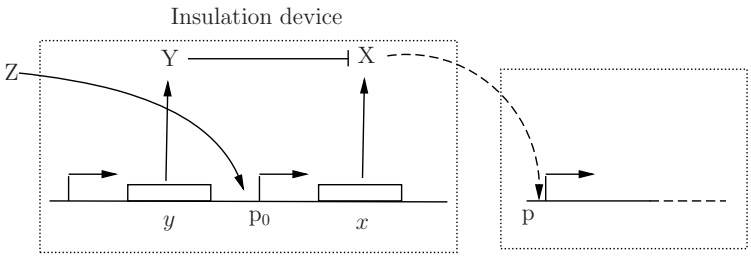

Figure 6.12: Implementation of high gain feedback (Design 1). The input $Z(t)$ is amplified by virtue of a strong promoter p_0. The negative feedback on the output X is obtained by enhancing its degradation through the protease Y.

the promoter p_0 controlling the expression of X is a strong, non-leaky promoter activated by Z. The signal $Z(t)$ can be further amplified by increasing the strength of the ribosome binding site of gene x. The negative feedback mechanism on X relies on enhanced degradation of X. Since this must be large, one possible way to obtain an enhanced degradation for X is to have a specific protease, called Y, be expressed by a strong constitutive promoter.

To investigate whether such a design realizes a large amplification and a large negative feedback on X as needed to attenuate retroactivity to the output, we construct a model. The reaction of the protease Y with protein X is modeled as the two-step reaction

$$\mathrm{X} + \mathrm{Y} \underset{d}{\overset{a}{\rightleftharpoons}} \mathrm{W} \overset{\bar{k}}{\rightarrow} \mathrm{Y}.$$

The input/output system model of the insulation device that takes Z as an input and gives X as an output is given by the following equations

$$\frac{dZ}{dt} = k(t) - \gamma_Z Z + \left[k'_{\mathrm{off}}\,\bar{C} - k'_{\mathrm{on}}\,Z(p_{0,\mathrm{tot}} - \bar{C})\right], \tag{6.12}$$

$$\frac{d\bar{C}}{dt} = k'_{\mathrm{on}} Z(p_{0,\mathrm{tot}} - \bar{C}) - k'_{\mathrm{off}}\bar{C}, \tag{6.13}$$

$$\frac{dm_X}{dt} = G\bar{C} - \delta m_X, \tag{6.14}$$

$$\frac{dW}{dt} = aXY - dW - \bar{k}W, \tag{6.15}$$

$$\frac{dY}{dt} = -aYX + \bar{k}W + \alpha G - \gamma_Y Y + dW, \tag{6.16}$$

$$\frac{dX}{dt} = \kappa m_X - aYX + dW - \gamma_X X + \left[k_{\mathrm{off}}C - k_{\mathrm{on}}X(p_{\mathrm{tot}} - C)\right], \tag{6.17}$$

$$\frac{dC}{dt} = -k_{\mathrm{off}}C + k_{\mathrm{on}}X(p_{\mathrm{tot}} - C), \tag{6.18}$$

in which we have assumed that the expression of gene z is controlled by a promoter with activity $k(t)$. In this system, we have denoted by k'_{on} and k'_{off} the association

and dissociation rate constants of Z with its promoter site p_0 in total concentration $p_{0,\text{tot}}$. Also, $\bar{C}$ is the complex of Z with such a promoter site. Here, m_X is the mRNA of X, and C is the complex of X bound to the downstream binding sites p with total concentration p_{tot}. The promoter controlling gene y has strength αG, for some constant α, and it has about the same strength as the promoter controlling gene x.

The terms in the square brackets in equation (6.12) represent the retroactivity r to the input of the insulation device in Figure 6.12. The terms in the square brackets in equation (6.17) represent the retroactivity s to the output of the insulation device. The dynamics of equations (6.12)–(6.18) without s describe the dynamics of X with no downstream system (isolated system).

Equations (6.12) and (6.13) determine the signal $\bar{C}(t)$ that is the input to equations (6.14)–(6.18). For the discussion regarding the attenuation of the effect of s, it is not relevant what the specific form of signal $\bar{C}(t)$ is. Let then $\bar{C}(t)$ be any bounded signal. Since equation (6.14) takes $\bar{C}(t)$ as an input, we will have that $m_X(t) = Gv(t)$, for a suitable signal $v(t)$. Let us assume for the sake of simplifying the analysis that the protease reaction is a one step reaction. Therefore, equation (6.16) simplifies to

$$\frac{dY}{dt} = \alpha G - \gamma_Y Y$$

and equation (6.17) simplifies to

$$\frac{dX}{dt} = \kappa m_X - \bar{k}' YX - \gamma_X X + k_{\text{off}} C - k_{\text{on}} X(p_{\text{tot}} - C),$$

for a suitable positive constant $\bar{k}'$. If we further consider the protease to be at its equilibrium, we have that $Y(t) = \alpha G/\gamma_Y$.

As a consequence, the X dynamics become

$$\frac{dX}{dt} = \kappa G v(t) - (\bar{k}' \alpha G/\gamma_Y + \gamma_X)X + k_{\text{off}} C - k_{\text{on}} X(p_{\text{tot}} - C),$$

with C determined by equation (6.18). By using the same singular perturbation argument employed in the previous section, the dynamics of X can be reduced to

$$\frac{dX}{dt} = (\kappa G v(t) - (\bar{k}' \alpha G/\gamma_Y + \gamma_X)X)(1 - d(t)), \tag{6.19}$$

in which $0 < d(t) < 1$ is the retroactivity term given by $\mathcal{R}(X)/(1 + \mathcal{R}(X))$. Then, as G increases, $X(t)$ becomes closer to the solution of the isolated system

$$\frac{dX}{dt} = \kappa G v(t) - (\bar{k}' \alpha G/\gamma_Y + \gamma_X)X,$$

as explained in the previous section be virtue of Proposition 6.1.

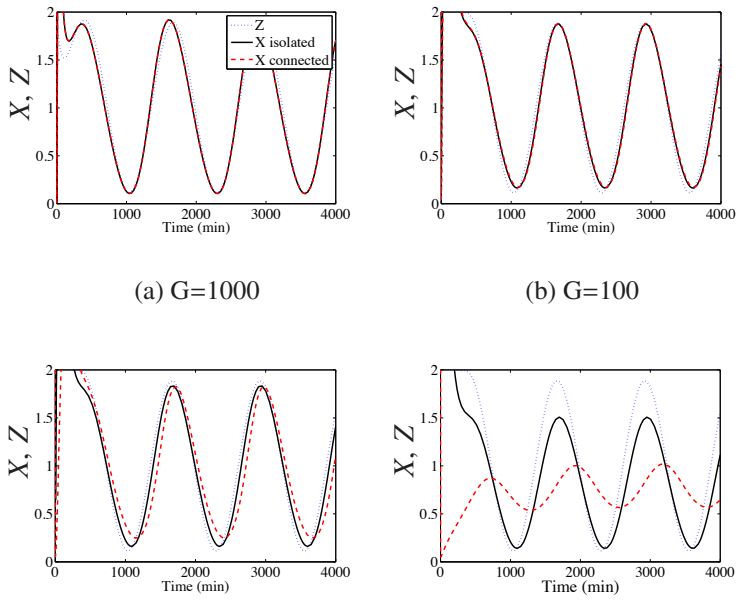

(a) G=1000 (b) G=100

(c) G=10 (d) G=1

Figure 6.13: Design 1: results for different gains G. In all plots, $k(t) = 0.01(1 + sin(\omega t))$, $p_{\text{tot}} = 100$ nM, $k_{\text{off}} = 10$ min^{-1}, $k_{\text{on}} = 10$ min^{-1} nM^{-1}, $\gamma_Z = 0.01 = \gamma_Y$ min^{-1}, and $\omega = 0.005$ rad/min. Also, we have set $\delta = 0.01$ min^{-1}, $p_{0,\text{tot}} = 1$ nM, $a = 0.01$ min^{-1} nM^{-1}, $d = \bar{k}' = 0.01$ min^{-1}, $k'_{\text{off}} = 200$ min^{-1}, $k'_{\text{on}} = 10$ min^{-1} nM^{-1}, $\alpha = 0.1$ nM/min, $\gamma_X = 0.1$ min^{-1}, $\kappa = 0.1$ min^{-1}, and $G = 1000, 100, 10, 1$. The retroactivity to the output is not well attenuated for values of the gain $G = 1$ and the attenuation capability begins to worsen for $G = 10$.

We now turn to the question of minimizing the retroactivity to the input r because its effect can alter the input signal $Z(t)$. In order to decrease r, we must guarantee that the retroactivity measure given in equation (6.6), in which we substitute Z in place of X, $p_{0,\text{tot}}$ in place of p_{tot}, and $K'_{\text{d}} = k'_{\text{on}}/k'_{\text{off}}$ in place of K_{d}, is small. This is the case if $K'_{\text{d}} \gg Z$ and $p_{0,\text{tot}}/K'_{\text{d}} \ll 1$.

Simulation results for the system described by equations (6.12)–(6.18) are shown in Figure 6.13. For large gains ($G = 1000$, $G = 100$), the performance considerably improves compared to the case in which X was generated by a transcriptional component accepting Z as an input (Figure 6.5). For lower gains ($G = 10$, $G = 1$), the performance starts to degrade for $G = 10$ and becomes poor for $G = 1$. Since we can view G as the number of transcripts produced per unit time (one minute) per complex of protein Z bound to promoter p_0, values $G = 100, 1000$ may be difficult to realize *in vivo*, while the values $G = 10, 1$ could be more easily realized. However, the value of κ increases with the strength of the ribosome binding site and therefore the gain may be further increased by picking strong ribosme binding

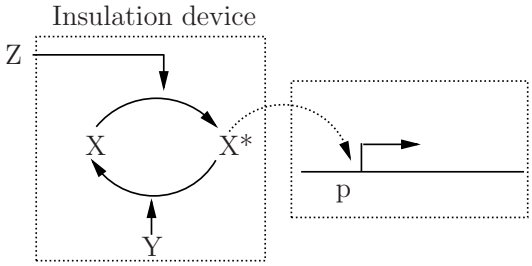

Figure 6.14: Implementation of high gain feedback (Design 2). Amplification of Z occurs through the phosphorylation of substrate X. Negative feedback occurs through a phosphatase Y that converts the active form X^* back to its inactive form X.

sites for x. The values of the parameters chosen in Figure 6.13 are such that $K'_d \gg Z$ and $p_{0,tot} \ll K'_d$. This is enough to guarantee that there is small retroactivity r to the input of the insulation device independently of the value of the gain G. The poorer performance of the device for $G = 1$ is therefore entirely due to poor attenuation of the retroactivity s to the output. To obtain a large negative feedback gain, we also require high expression of the protease. It is therefore important that the protease is highly specific to its target X.

Design 2: Amplification through phosphorylation

In this design, the amplification gain G of Z is obtained by having Z be a kinase that phosphorylates a substrate X, which is available in abundance. The negative feedback gain G' on the phosphorylated protein X^* is obtained by having a phosphatase Y dephosphorylate the active protein X^*. Protein Y should also be available in abundance in the system. This implementation is depicted in Figure 6.14.

To illustrate what key parameters enable retroactivity attenuation, we first consider a simplified model for the phosphorylation and dephosphorylation processes. This model will help in obtaining a conceptual understanding of what reactions are responsible in realizing the desired gains G and G'. The one step model that we consider is the same as considered in Chapter 2 (Exercise 2.12):

$$Z + X \xrightarrow{k_1} Z + X^*, \qquad Y + X^* \xrightarrow{k_2} Y + X.$$

We assume that there is an abundance of protein X and of phosphatase Y in the system and that these quantities are conserved. The conservation of X gives $X + X^* + C = X_{tot}$, in which X is the inactive protein, X^* is the phosphorylated protein that binds to the downstream sites p, and C is the complex of the phosphorylated

protein X^* bound to the promoter p. The X^* dynamics can be described by the following model

$$\begin{aligned}\frac{dX^*}{dt} &= k_1 X_{\text{tot}} Z(t)\left(1 - \frac{X^*}{X_{\text{tot}}} - \left[\frac{C}{X_{\text{tot}}}\right]\right) - k_2 Y X^* + [k_{\text{off}} C - k_{\text{on}} X^*(p_{\text{tot}} - C)],\\ \frac{dC}{dt} &= -k_{\text{off}} C + k_{\text{on}} X^*(p_{\text{tot}} - C).\end{aligned} \tag{6.20}$$

The two terms in the square brackets represent the retroactivity s to the output of the insulation device of Figure 6.14. For a weakly activated pathway [41], $X^* \ll X_{\text{tot}}$. Also, if we assume that the total concentration of X is large compared to the concentration of the downstream binding sites, that is, $X_{\text{tot}} \gg p_{\text{tot}}$, equation (6.20) is approximatively equal to

$$\frac{dX^*}{dt} = k_1 X_{\text{tot}} Z(t) - k_2 Y X^* + k_{\text{off}} C - k_{\text{on}} X^*(p_{\text{tot}} - C).$$

Let $G = k_1 X_{\text{tot}}$ and $G' = k_2 Y$. Exploiting again the difference of time scales between the X^* dynamics and the C dynamics, the dynamics of X^* can be finally reduced to

$$\frac{dX^*}{dt} = (GZ(t) - G'X^*)(1 - d(t)),$$

in which $0 < d(t) < 1$ is the retroactivity term. Therefore, for G and G' large enough, $X^*(t)$ tends to the solution $X^*(t)$ of the isolated system

$$\frac{dX^*}{dt} = GZ(t) - G'X^*,$$

as explained before by virtue of Proposition 6.1. It follows that the effect of the retroactivity to the output s is attenuated by increasing the effective rates $k_1 X_{\text{tot}}$ and $k_2 Y$. That is, to obtain large input and negative feedback gains, one should have large phosphorylation/dephosphorylation rates and/or a large amount of protein X and phosphatase Y in the system. This reveals that the values of the phosphorylation/dephosphorylation rates cover an important role toward the retroactivity attenuation property of the module of Figure 6.14. From a practical point of view, the effective rates can be increased by increasing the total amounts of X and Y. These amounts can be tuned, for example, by placing the x and y genes under the control of inducible promoters. The reader can verify through simulation how increasing the phosphatase and substrate amounts the effect of retroactivity can be attenuated (see Exercise 6.9). Experiments performed on a covalent modification cycle reconstituted *in vitro* confirmed that increasing the effective rates of modification is an effective means to attain retroactivity attenuation [50].

A design similar to the one illustrated here can be proposed in which a phosphorylation cascade, such as the MAPK cascade, realizes the input amplification and an explicit feedback loop is added from the product of the cascade to its input

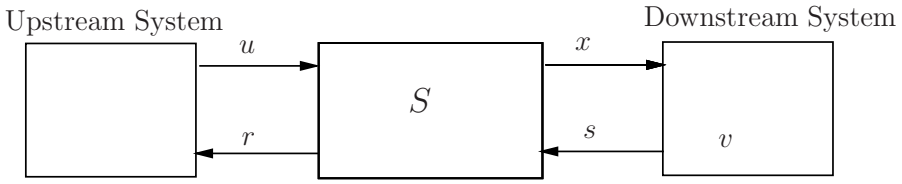

Figure 6.15: Interconnection of a device with input u and output x to a downstream system with internal state v applying retroactivity s.

[81]. The design presented here is simpler as it involves only one phosphorylation cycle and does not require any explicit feedback loop. In fact, a strong negative feedback can be realized by the action of the phosphatase that converts the active protein form X^* back to its inactive form X.

Attenuation of retroactivity to the output using time-scale separation

In this section, we present a more general mechanism for retroactivity attenuation, which can be applied to systems of differential equations of arbitrary dimension. This will allow us to consider more complex and realistic models of the phosphorylation reactions as well as more complicated systems.

For this purpose, consider Figure 6.15. We illustrate next how system S can attenuate retroactivity s by employing the principle of time scale separation. Specifically, when the internal dynamics of the system are much faster compared to the input u, the system immediately reaches its quasi-steady state with respect to the input. This quasi-steady state, in turn, is basically independent of s due to the interconnection structure between the systems. To illustrate this idea mathematically, consider the following simple structure in which (for simplicity) we assume that all variables are scalar:

$$\frac{du}{dt} = f_0(u,t) + r(u,x), \qquad \frac{dx}{dt} = Gf_1(x,u) + \bar{G}s(x,v), \qquad \frac{dv}{dt} = -\bar{G}s(x,v). \quad (6.21)$$

Here let $G \gg 1$ model the fact that the internal dynamics of the system are much faster than that of the input. Similarly, $\bar{G} \gg 1$ models the fact that the dynamics of the interconnection with downstream systems are also very fast. This is usually the case since the reactions contributing to s are usually binding/unbinding reactions, which are much faster than most of other biochemical processes, including gene expression and phosphorylation. We make the following informal claim:

> If $G \gg 1$ and the Jacobian $\partial f_1(x,u)/\partial x$ has eigenvalues with negative real part, then $x(t)$ is not affected by retroactivity s after a short initial transient, independently of the value of $\bar{G}$.

A formal statement of this result can be found in [48]. This result states that independently of the characteristics of the downstream system, system S can be tuned

(by making G large enough) such that it attenuates the retroactivity to the output. To clarify why this would be the case, it is useful to rewrite system (6.21) in standard singular perturbation form by employing $\epsilon := 1/G$ as a small parameter and $\tilde{x} := x + v$ as the slow variable. Hence, the dynamics can be rewritten as

$$\frac{du}{dt} = f_0(u,t) + r(u,x), \qquad \epsilon\frac{d\tilde{x}}{dt} = f_1(\tilde{x}-v,u), \qquad \frac{dv}{dt} = -\bar{G}s(\tilde{x}-v,v). \tag{6.22}$$

Since $\partial f_1/\partial\tilde{x}$ has eigenvalues with negative real part, one can apply standard singular perturbation to show that after a very fast transient, the trajectories are attracted to the slow manifold given by $f_1(\tilde{x}-v,u) = 0$. This is locally given by $x = g(u)$ solving $f_1(x,u) = 0$. Hence, on the slow manifold we have that $x(t) = g(u(t))$, which is independent of the downstream system, that is, it is not affected by retroactivity.

The same result holds for a more general class of systems in which the variables u, x, v are vectors:

$$\frac{du}{dt} = f_0(u,t) + r(u,x), \qquad \frac{dx}{dt} = Gf_1(x,u) + \bar{G}As(x,v), \qquad \frac{dv}{dt} = -\bar{G}Bs(x,v) \tag{6.23}$$

as long as there are matrices T and M such that $TA - MB = 0$ and T is invertible. In fact, one can take the system to new coordinates $u, \tilde{x}, v$ with $\tilde{x} = Tx + Mv$, in which the system will have the singular perturbation form (6.22), where the state variables are vectors. Note that matrices A and B are stoichiometry matrices and s represents a vector of reactions, usually modeling binding and unbinding processes. The existence of T and M such that $TA - MB = 0$ models the fact that in these binding reactions species do not get destroyed or created, but simply transformed between species that belong to the upstream system and species that belong to the downstream system.

Biomolecular realizations of time-scale separation

We next consider possible biomolecular structures that realize the time-scale separation required for insulation. Since this principle is based on a fast time scale of the device dynamics when compared to that of the device input, we focus on signaling systems, which are known to evolve on faster time scales than those of protein production and decay.

Design 1: Implementation through phosphorylation

We consider now a more realistic model for the phosphorylation and dephosphorylation reactions in a phosphorylation cycle than those considered in Section 6.5. In particular, we consider a two-step reaction model as seen in Section 2.4. According to this model, we have the following two reactions for phosphorylation and

dephosphorylation:

$$\mathrm{Z}+\mathrm{X} \underset{d_1}{\overset{a_1}{\rightleftharpoons}} \mathrm{C}_1 \xrightarrow{k_1} \mathrm{X}^*+\mathrm{Z}, \qquad \mathrm{Y}+\mathrm{X}^* \underset{d_2}{\overset{a_2}{\rightleftharpoons}} \mathrm{C}_2 \xrightarrow{k_2} \mathrm{X}+\mathrm{Y}. \tag{6.24}$$

Additionally, we have the conservation equations $Y_{\mathrm{tot}} = Y + C_2$, $X_{\mathrm{tot}} = X + X^* + C_1 + C_2 + C$, because proteins X and Y are not degraded. Therefore, the differential equations modeling the system of Figure 6.14 become

$$\frac{dZ}{dt} = k(t) - \gamma Z\left[-a_1 Z X_{\mathrm{tot}}\left(1 - \frac{X^*}{X_{\mathrm{tot}}} - \frac{C_1}{X_{\mathrm{tot}}} - \frac{C_2}{X_{\mathrm{tot}}} - \left[\frac{C}{X_{\mathrm{tot}}}\right]\right) + (d_1 + k_1)C_1\right], \tag{6.25}$$

$$\frac{dC_1}{dt} = -(d_1 + k_1)C_1 + a_1 Z X_{\mathrm{tot}}\left(1 - \frac{X^*}{X_{\mathrm{tot}}} - \frac{C_1}{X_{\mathrm{tot}}} - \frac{C_2}{X_{\mathrm{tot}}} - \left[\frac{C}{X_{\mathrm{tot}}}\right]\right), \tag{6.26}$$

$$\frac{dC_2}{dt} = -(k_2 + d_2)C_2 + a_2 Y_{\mathrm{tot}} X^*\left(1 - \frac{C_2}{Y_{\mathrm{tot}}}\right), \tag{6.27}$$

$$\frac{dX^*}{dt} = k_1 C_1 + d_2 C_2 - a_2 Y_{\mathrm{tot}} X^*\left(1 - \frac{C_2}{Y_{\mathrm{tot}}}\right) + \left[k_{\mathrm{off}} C - k_{\mathrm{on}} X^*(p_{\mathrm{tot}} - C)\right], \tag{6.28}$$

$$\frac{dC}{dt} = -k_{\mathrm{off}} C + k_{\mathrm{on}} X^*(p_{\mathrm{tot}} - C), \tag{6.29}$$

in which the production of Z is controlled by a promoter with activity $k(t)$. The terms in the large square bracket in equation (6.25) represent the retroactivity r to the input, while the terms in the square brackets of equations (6.26) and (6.28) represent the retroactivity s to the output.

We assume that $X_{\mathrm{tot}} \gg p_{\mathrm{tot}}$ so that in equations (6.25) and (6.26) we can neglect the term C/X_{tot} since $C < p_{\mathrm{tot}}$. Choose X_{tot} to be sufficiently large so that $G = a_1 X_{\mathrm{tot}}/\gamma \gg 1$. Also, let $\bar{G} = k_{\mathrm{off}}/\gamma$, which is also much larger than 1 since binding reactions are much faster than protein production and decay rates ($k_{\mathrm{off}} \gg \gamma$) and write $k_{\mathrm{on}} = k_{\mathrm{off}}/K_{\mathrm{d}}$. Choosing Y_{tot} to also be sufficiently large, we can guarantee that $a_2 Y_{\mathrm{tot}}$ is of the same order as $a_1 X_{\mathrm{tot}}$ and we can let $\alpha_1 = a_1 X_{\mathrm{tot}}/(\gamma G)$, $\alpha_2 = a_2 Y_{\mathrm{tot}}/(\gamma G)$, $\delta_1 = d_1/(\gamma G)$, and $\delta_2 = d_2/(\gamma G)$. Finally, since the catalytic rates k_1, k_2 are much larger than protein decay, we can assume that they are of the same order of magnitude as $a_1 X_{\mathrm{tot}}$ and $a_2 Y_{\mathrm{tot}}$, so that we define $c_i = k_i/(\gamma G)$. With these, letting

$z = Z + C_1$ we obtain the system in the form

$$\begin{aligned}
\frac{dz}{dt} &= k(t) - \gamma(z - C_1),\\
\frac{dC_1}{dt} &= G\left(-\gamma(\delta_1 + c_1)C_1 + \gamma\alpha_1(z - C_1)\left(1 - \frac{X^*}{X_{\text{tot}}} - \frac{C_1}{X_{\text{tot}}} - \frac{C_2}{X_{\text{tot}}}\right)\right),\\
\frac{dC_2}{dt} &= G\left(-\gamma(\delta_2 + c_2)C_2 + \gamma\alpha_2 X^*\left(1 - \frac{C_2}{Y_{\text{tot}}}\right)\right),\\
\frac{dX^*}{dt} &= G\left(\gamma c_1 C_1 + \gamma\delta_2 C_2 - \gamma\alpha_2 X^*\left(1 - \frac{C_2}{Y_{\text{tot}}}\right)\right) + \bar{G}\left(\gamma C - \gamma/K_{\text{d}}(p_{\text{tot}} - C)X^*\right),\\
\frac{dC}{dt} &= -\bar{G}\left(\gamma C - \gamma/K_{\text{d}}(p_{\text{tot}} - C)X^*\right),
\end{aligned} \tag{6.30}$$

which is in the form of system (6.23) with $u = z$, $x = (C_1, C_2, X^*)$, and $v = C$, in which one can choose T as the 3×3 identity matrix and

$$M = \begin{pmatrix} 0 \\ 0 \\ 1 \end{pmatrix}.$$

It is also possible to show that the Jacobian of f_1 has eigenvalues with negative real part (see Exercise 6.11). Hence, for G sufficiently larger than 1, this system attenuates the effect of the retroactivity to the output s. For G to be large, one has to require that $a_1 X_{\text{tot}}$ is sufficiently large and that $a_2 Y_{\text{tot}}$ is also comparatively large. These are compatible with the design requirements obtained in the previous section based on the one-step reaction model of the enzymatic reactions.

In order to understand the effect of retroactivity to the input on the Z dynamics, one can consider the reduced system describing the dynamics on the time scale of Z. To this end, let $K_{m,1} = (d_1 + k_1)/a_1$ and $K_{m,2} = (d_2 + k_2)/a_2$ represent the Michaelis-Menten constants of the forward and backward enzymatic reactions, let $G = 1/\epsilon$ in equations (6.30), and take ϵ to the left-hand side. Setting $\epsilon = 0$, the following relationships can be obtained:

$$C_1 = g_1(X^*) = \frac{(X^* Y_{\text{tot}} k_2)/(K_{m,2} k_1)}{1 + X^*/K_{m,2}}, \qquad C_2 = g_2(X^*) = \frac{(X^* Y_{\text{tot}})/K_{m,2}}{1 + X^*/K_{m,2}}. \tag{6.31}$$

Using expressions (6.31) in the second of equations (6.30) with $\epsilon = 0$ leads to

$$g_1(X^*)\left(\delta_1 + c_1 + \frac{\alpha_1 Z}{X_{\text{tot}}}\right) = \alpha_1 Z\left(1 - \frac{X^*}{X_{\text{tot}}} - \frac{g_2(X^*)}{X_{\text{tot}}}\right). \tag{6.32}$$

Assuming for simplicity that $X^* \ll K_{m,2}$, we obtain that

$$g_1(X^*) \approx (X^* Y_{\text{tot}} k_2)/(K_{m,2} k_1)$$

and that

$$g_2(X^*) \approx X^*/K_{m,2}Y_{\text{tot}}.$$

As a consequence of these simplifications, equation (6.32) leads to

$$X^*(Z) = \frac{\alpha_1 Z}{(\alpha_1 Z/X_{\text{tot}})(1 + Y_{\text{tot}}/K_{m,2} + (Y_{\text{tot}}k_2)/(K_{m,2}k_1)) + (Y_{\text{tot}}k_2)/(K_{m,2}k_1)(\delta_1 + c_1)}.$$

In order not to have distortion from Z to X^*, we require that

$$Z \ll \frac{Y_{\text{tot}}(k_2/k_1)(K_m/K_{m,2})}{1 + Y_{\text{tot}}/K_{m,2} + (Y_{\text{tot}}/K_{m,2})(k_2/k_1)}, \tag{6.33}$$

so that $X^*(Z) \approx Z(X_{\text{tot}}K_{m,2}k_1)/(Y_{\text{tot}}K_{m,1}k_2)$ and therefore we have a linear relationship between X^* and Z with gain from Z to X^* given by $(X_{\text{tot}}K_{m,2}k_1)/(Y_{\text{tot}}K_{m,1}k_2)$. In order not to have attenuation from Z to X^* we require that the gain is greater than or equal to one, that is,

$$\text{input/output gain} \approx \frac{X_{\text{tot}}K_{m,2}k_1}{Y_{\text{tot}}K_{m,1}k_2} \geq 1. \tag{6.34}$$

Requirements (6.33), (6.34) and $X^* \ll K_{m,2}$ are enough to guarantee that we do not have nonlinear distortion between Z and X^* and that X^* is not attenuated with respect to Z. In order to guarantee that the retroactivity r to the input is sufficiently small, we need to quantify the retroactivity effect on the Z dynamics due to the binding of Z with X. To achieve this, we proceed as in Section 6.3 by computing the Z dynamics on the slow manifold, which gives a good approximation of the dynamics of Z if $\epsilon \approx 0$. These dynamics are given by

$$\frac{dZ}{dt} = (k(t) - \gamma Z)\left(1 - \frac{dg_1}{dX^*}\frac{dX^*}{dz}\right),$$

in which $(dg_1/dX^*)(dX^*/dz)$ measures the effect of the retroactivity r to the input on the Z dynamics. Direct computation of dg_1/dX^* and of dX^*/dz along with $X^* \ll K_{m,2}$ and with (6.33) leads to $(dg_1/dX^*)(dX^*/dz) \approx X_{\text{tot}}/K_{m,1}$, so that in order to have small retroactivity to the input, we require that

$$\frac{X_{\text{tot}}}{K_{m,1}} \ll 1. \tag{6.35}$$

Hence, a design trade-off appears: X_{tot} should be sufficiently large to provide a gain G large enough to attenuate the retroactivity to the output. Yet, X_{tot} should be small enough compared to $K_{m,1}$ so to apply minimal retroactivity to the input.

In conclusion, in order to have attenuation of the effect of the retroactivity to the output s, we require that the time scale of the phosphorylation/dephosphorylation reactions is much faster than the production and decay processes of Z (the input

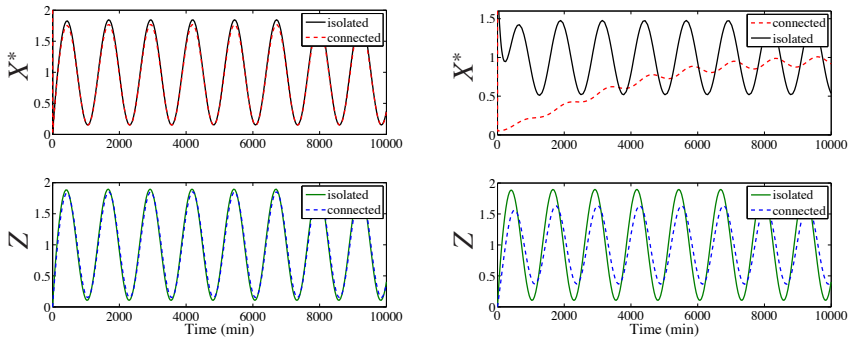

(a) Fast cycle (b) Slow cycle

Figure 6.16: Time-scale separation mechanism for insulation: Implementation through phosphorylation. Simulation results for system in equations (6.25)–(6.29). In all plots, $p_{\text{tot}} = 100$ nM, $k_{\text{off}} = 10$ min^{-1}, $k_{\text{on}} = 10$ min^{-1} nM^{-1}, $\gamma = 0.01$ min^{-1}, $k(t) = 0.01(1 + sin(\omega t))$ min^{-1}, and $\omega = 0.005$ rad/min. (a) Performance with fast phosphorylation cycle. Here, $k_1 = k_2 = 50$ min^{-1}, $a_2 = a_1 = 0.01$ min^{-1} nM^{-1} , $d_1 = d_2 = 10$ min^{-1}, and $Y_{\text{tot}} = X_{\text{tot}} = 1500$ nM. The small error shows that the effect of the retroactivity to the output s is attenuated very well. In the Z plot, the isolated system stands for the case in which Z does not have X to bind to, while the connected system stands for the case in which Z binds to substrate X. The small error confirms a small retroactivity to the input r. (b) Performance with a slow phosphorylation cycle. Here, we set $k_1 = k_2 = 0.01$ min^{-1}, while the other parameters are left the same.

to the insulation device) and that $X_{\text{tot}} \gg p_{\text{tot}}$, that is, the total amount of protein X is in abundance compared to the downstream binding sites p. To also obtain a small effect of the retroactivity to the input, we require that $K_{m,1} \gg X_{\text{tot}}$. This is satisfied if, for example, kinase Z has low affinity to binding with X. To keep the input/output gain between Z and X^* close to one (from equation (6.34)), one can choose $X_{\text{tot}} = Y_{\text{tot}}$, and equal coefficients for the phosphorylation and dephosphorylation reactions, that is, $K_{m,1} = K_{m,2}$ and $k_1 = k_2$.

The system in equations (6.25)–(6.29) was simulated with and without the downstream binding sites p, that is, with and without, respectively, the terms in the small box of equation (6.25) and in the boxes in equations (6.28) and (6.26). This is performed to highlight the effect of the retroactivity to the output s on the dynamics of X^*. The simulations validate our theoretical study that indicates that when $X_{\text{tot}} \gg p_{\text{tot}}$ and the time scales of phosphorylation/dephosphorylation are much faster than the time scale of decay and production of the protein Z, the retroactivity to the output s is very well attenuated (Figure 6.16a). Similarly, the time behavior of Z was simulated with and without the terms in the square brackets in equation (6.25), which represent the retroactivity to the input r, to verify whether the insulation device exhibits small retroactivity to the input r. The similarity of the behaviors of $Z(t)$ with and without its downstream binding sites on X

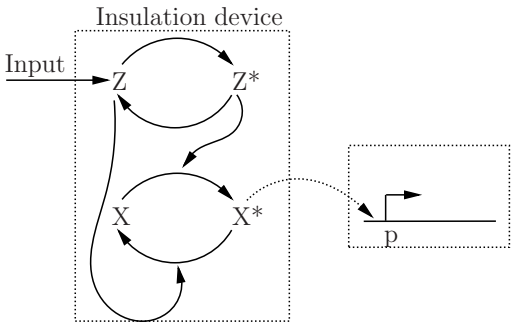

Figure 6.17: The insulation device is a phosphotransfer system. The output X^* activates transcription through the reversible binding of X^* to downstream DNA promoter sites p.

(Figure 6.16a) indicates that there is no substantial retroactivity to the input r generated by the insulation device. This is obtained because $X_{\text{tot}} \ll K_{m,1}$ as indicated in equation (6.35), in which $1/K_m$ can be interpreted as the affinity of the binding of X to Z.

Our simulation study also indicates that a faster time scale of the phosphorylation/dephosphorylation reactions is necessary, even for high values of X_{tot} and Y_{tot}, to maintain perfect attenuation of the retroactivity to the output s and small retroactivity to the output r. In fact, slowing down the time scale of phosphorylation and dephosphorylation, the system looses its insulation property (Figure 6.16b). In particular, the attenuation of the effect of the retroactivity to the output s is lost because there is not enough separation of time scales between the Z dynamics and the internal device dynamics. The device also displays a non negligible amount of retroactivity to the input because the condition $K_m \ll X_{\text{tot}}$ is not satisfied anymore.

Design 2: Realization through phosphotransfer

Here we illustrate that another possible implementation of the mechanism for insulation based on time-scale separation is provided by phosphotransfer systems. These systems, just like phosphorylation cycles, have a very fast dynamics when compared to gene expression. Specifically, we consider the realization shown in Figure 6.17, in which the input is a phosphate donor Z and the output is the active transcription factor X^*. We let X be the transcription factor in its inactive form and let Z^* be the active phosphate donor, that is, a protein that can transfer its phosphate group to the acceptor X. The standard phosphotransfer reactions can be modeled according to the two-step reaction model

$$Z^* + X \underset{k_2}{\overset{k_1}{\rightleftharpoons}} C_1 \underset{k_4}{\overset{k_3}{\rightleftharpoons}} X^* + Z,$$

in which C_1 is the complex of Z bound to X bound to the phosphate group. Additionally, we assume that protein Z can be phosphorylated and protein X^* dephosphorylated by other phosphotransfer interactions. These reactions are modeled as one-step reactions depending only on the concentrations of Z and X^*, that is,

$$Z \xrightarrow{\pi_1} Z^*, \qquad X^* \xrightarrow{\pi_2} X.$$

Protein X is assumed to be conserved in the system, that is, $X_{\text{tot}} = X + C_1 + X^* + C$. We assume that protein Z is produced with time-varying production rate $k(t)$ and decays with rate γ. The active transcription factor X^* binds to downstream DNA binding sites p with total concentration p_{tot} to activate transcription through the reversible reaction

$$p + X^* \underset{k_{\text{off}}}{\overset{k_{\text{on}}}{\rightleftharpoons}} C.$$

Since the total amount of p is conserved, we also have that $C + p = p_{\text{tot}}$. The ODE model corresponding to this system is thus given by the equations

$$\begin{aligned}
\frac{dZ}{dt} &= k(t) - \gamma Z + k_3 C_1 - k_4 X^* Z - \pi_1 Z, \\
\frac{dC_1}{dt} &= k_1 X_{\text{tot}} \left(1 - \frac{X^*}{X_{\text{tot}}} - \frac{C_1}{X_{\text{tot}}} - \left[\frac{C}{X_{\text{tot}}}\right]\right) Z^* - k_3 C_1 - k_2 C_1 + k_4 X^* Z, \\
\frac{dZ^*}{dt} &= \pi_1 Z + k_2 C_1 - k_1 X_{\text{tot}} \left(1 - \frac{X^*}{X_{\text{tot}}} - \frac{C_1}{X_{\text{tot}}} - \left[\frac{C}{X_{\text{tot}}}\right]\right) Z^*, \\
\frac{dX^*}{dt} &= k_3 C_1 - k_4 X^* Z + \left[k_{\text{off}} C - k_{\text{on}} X^* (p_{\text{tot}} - C)\right] - \pi_2 X^*, \\
\frac{dC}{dt} &= k_{\text{on}} X^* (p_{\text{tot}} - C) - k_{\text{off}} C.
\end{aligned} \tag{6.36}$$

Just like phosphorylation, phosphotransfer reactions are much faster than protein production and decay. Hence, as performed before, define $G = X_{\text{tot}} k_1/\gamma$ so that $\bar{k}_1 = X_{\text{tot}} k_1/G$, $\bar{k}_2 = k_2/G$, $\bar{k}_3 = k_3/G$, $\bar{k}_4 = X_{\text{tot}} k_4/G$, $\bar{\pi}_1 = \pi_1/G$, and $\bar{\pi}_2 = \pi_2/G$ are of the same order of $k(t)$ and γ. Similarly, the process of protein binding and unbinding to promoter sites is much faster than protein production and decay. We let $\bar{G} = k_{\text{off}}/\gamma$ and $K_{\text{d}} = k_{\text{off}}/k_{\text{on}}$. Assuming also that $p_{\text{tot}} \ll X_{\text{tot}}$, we have that $C \ll X_{\text{tot}}$

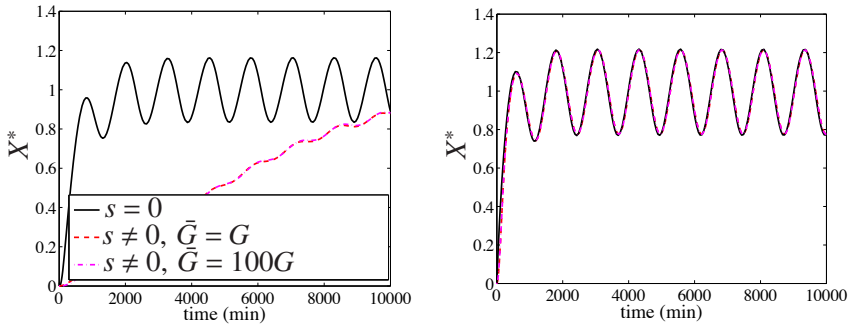

(a) $G = 1$ (b) $G = 100$

Figure 6.18: Output response of the phosphotransfer system with a periodic signal $k(t) = \gamma(1 + 0.5\sin\omega t)$. The parameters are given by $\gamma = 0.01$ min^{-1}, $X_{\text{tot}} = 5000$ nM, $k_1 = k_2 = k_3 = k_4 = 0.01$ min^{-1} nM^{-1}, $\pi_1 = \pi_2 = 0.01G$ min^{-1} in which $G = 1$ in (a), and $G = 100$ in (b). The downstream system parameters are given by $K_{\text{d}} = 1$ nM and $k_{\text{off}} = 0.01\bar{G}$ min^{-1}, in which $\bar{G}$ takes the values indicated on the legend. The isolated system ($s = 0$) corresponds to $p_{\text{tot}} = 0$ while the connected system ($s \neq 0$) corresponds to $p_{\text{tot}} = 100$ nM.

so that system (6.36) can be rewritten as

$$\begin{aligned}
\frac{dZ}{dt} &= k(t) - \gamma Z - G\bar{\pi}_1 Z + G\left(\bar{k}_3 C_1 - \bar{k}_4\left(\frac{X^*}{X_{\text{tot}}}\right)Z\right),\\
\frac{dC_1}{dt} &= G\left(\bar{k}_1\left(1 - \frac{X^*}{X_{\text{tot}}} - \frac{C_1}{X_{\text{tot}}}\right)Z^* - \bar{k}_3 C_1 - \bar{k}_2 C_1 + \bar{k}_4\left(\frac{X^*}{X_{\text{tot}}}\right)Z\right),\\
\frac{dZ^*}{dt} &= G\left(\bar{\pi}_1 Z + \bar{k}_2 C_1 - \bar{k}_1\left(1 - \frac{X^*}{X_{\text{tot}}} - \frac{C_1}{X_{\text{tot}}}\right)Z^*\right),\\
\frac{dX^*}{dt} &= G\left(\bar{k}_3 C_1 - \bar{k}_4\left(\frac{X^*}{X_{\text{tot}}}\right)Z - \bar{\pi}_2 X^*\right) + \bar{G}\left(\gamma C - \frac{\gamma}{K_{\text{d}}}X^*(p_{\text{tot}} - C)\right),\\
\frac{dC}{dt} &= -\bar{G}\left(\gamma C - \frac{\gamma}{K_{\text{d}}}X^*(p_{\text{tot}} - C)\right).
\end{aligned} \tag{6.37}$$

Taking $T = \mathbb{I}_{3\times 3}$, the 3×3 identity matrix, and

$$M = \begin{pmatrix} 0 \\ 0 \\ 1 \end{pmatrix},$$

the coordinate transformation $\tilde{x} = Tx + Mv$ brings the system to the form of system (6.23) with $u = Z$, $x = (C_1, Z^*, X^*)$, and $v = C$. The reader can verify that the Jacobian of $f_1(x,u)$ has eigenvalues with negative real part (Exercise 6.10).

Figure 6.18a shows that, for a periodic input $k(t)$, the system with low value for G suffers from retroactivity to the output. However, for a large value of G (Figure

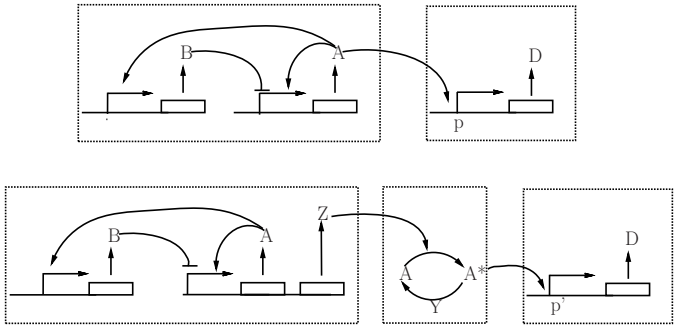

Figure 6.19: The activator-repressor clock connected to its downstream system through the insulation device of Figure 6.14. The top diagram illustrates a simplified genetic layout of the activator-repressor clock of Figure 6.2a. The bottom diagram illustrates how the genetic layout of the clock should be modified such that it can connect to the phosphorylation cycle that takes as input the kinase Z. In this case, the downstream system still expresses protein D, but its expression is controlled by a different promoter that is activated by X^* as opposed to being activated by A.

6.18b), the permanent behavior of the connected system becomes similar to that of the isolated system, whether $G \gg \bar{G}$, $G = \bar{G}$ or $G \ll \bar{G}$. This confirms the theoretical result that, independently of the order of magnitude of $\bar{G}$, the system can arbitrarily attenuate retroactivity for large enough G. Note that this robustness to the load applied on X^* is achieved even if the concentration of X^* is about 100 times smaller than the concentration of the load applied to it. This allows to design the system such that it can output any desired value while being robust to retroactivity.

6.6 A Case Study on the Use of Insulation Devices

In this section, we consider again the problem illustrated at the beginning of the chapter in which we would like to transmit the periodic stimulation of the activator-repressor clock to a downstream system (Figure 6.2b). We showed before that connecting the clock directly to the downstream system causes the oscillations to be attenuated and even quenched (Figure 6.2c), so that we fail to transmit the desired periodic stimulation to the downstream system. Here, we describe a solution to this problem that implements an insulation device to connect the clock to the downstream system. This way, the downstream system receives the desired periodic input stimulation despite the potentially large retroactivity s that this system applies to the insulation device. In particular, we employ the insulation device realized by a phosphorylation cycle in the configuration shown in Figure 6.19. The top diagram illustrates a simplified genetic layout of the clock. The activator A is expressed from a gene under the control of a promoter activated by A and repressed by B, while the repressor is expressed from a gene under the control of a

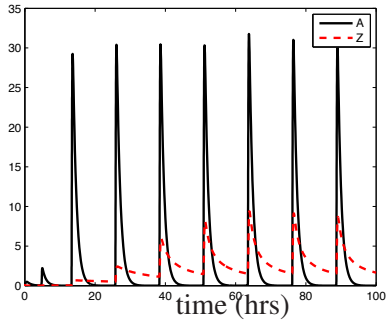

Figure 6.20: Simulation results for the concentration of protein Z in Figure 6.19 in the case in which this were used directly as an input to the downstream system, thus binding sites p' (dashed red plot). The clock parameters are the same as those in Figure 6.2c and $\gamma_K = \gamma_A$.

promoter activated by A. Protein A, in turn, activates the expression of protein D in the downstream system. In this case, the promoter p controlling the expression of D contains operator regions that A recognizes, so that A can bind to it.

When the insulation device of Figure 6.14 is employed to interconnect the clock to the downstream system, two modifications need to be made to enable the connections. Since A is not a kinase, we need to insert downstream of the gene expressing A another gene expressing the kinase Z (bottom diagram of Figure 6.19). Since both A and Z are under the control of the same promoter, they will be produced at the same rates and hence the concentration of Z should mirror that of A if the decay rates are the same for both proteins. Note that a solution in which we insert downstream of the gene expressing A a transcription factor Z that directly binds to downstream promoter sites p' to produce D (without the insulation device in between) would not solve the problem. In fact, while the clock behavior would be preserved in this case, the behavior of the concentration of Z would not mirror that of A since protein Z would be loaded by the downstream promoter sites p' (Figure 6.20). As a consequence, we would still fail to transmit the clock signal $A(t)$ to protein D. The second modification that needs to be made is to change the promoter p to a new promoter p' that has an operator that protein X^* recognizes (bottom diagram of Figure 6.19).

In the case of the bottom diagram of Figure 6.19, the dynamics of the clock proteins remain the same as that of model (5.11) and given by

$$\begin{aligned}\frac{dA}{dt} &= \frac{\kappa_A}{\delta_A}\frac{\alpha_A(A/K_A)^n + \alpha_{A0}}{1 + (A/K_A)^n + (B/K_B)^m} - \gamma_A A,\\ \frac{dB}{dt} &= \frac{\kappa_B}{\delta_B}\frac{\alpha_B(A/K_A)^n + \alpha_{B0}}{1 + (A/K_A)^n} - \gamma_B B.\end{aligned}$$

To these equations, we need to add the dynamics of the kinase $Z(t)$, which, when

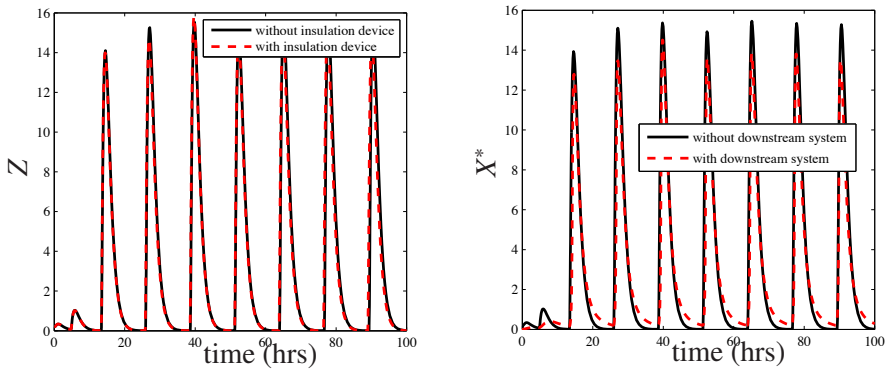

(a) (b)

Figure 6.21: Simulation results for the system of Figure 6.19. Panel (a) shows the concentration of the kinase Z with and without ($r = 0$ in equation (6.25)) the insulation device. Panel (b) shows the behavior of the output of the insulation device X^* without ($s = 0$) and with the downstream system. The clock parameters are the same as those in Figure 6.2c and $\gamma_K = \gamma_A$. The phosphorylation cycle parameters are as in Figure 6.16a. The load parameters are given by $k_{\text{on}} = 50$ min^{-1} nM^{-1}, $k_{\text{off}} = 50$ min^{-1}, and $p_{\text{tot}} = 100$ nM.

the phosphorylation cycle is not present, will be given by

$$\frac{dZ}{dt} = \frac{\kappa_A}{\delta_A} \frac{\alpha_A (A/K_A)^n + \alpha_{A0}}{1 + (A/K_A)^n + (B/K_B)^m} - \gamma_Z Z. \tag{6.38}$$

Note that we are using for simplicity the two-dimensional model of the activator-repressor clock. A similar result would be obtained using the four dimensional model that incorporates the mRNA dynamics (see Exercise 6.13).

When the phosphorylation cycle is present, the differential equation for Z given by (6.38) changes to

$$\begin{aligned} \frac{dZ}{dt} &= \frac{\kappa_A}{\delta_A} \frac{\alpha_A (A/K_A)^n + \alpha_{A0}}{1 + (A/K_A)^n + (B/K_B)^m} - \gamma_Z Z \\ &- \left[a_1 X_{\text{tot}} Z \left(1 - \frac{X^*}{X_{\text{tot}}} - \frac{C_1}{X_{\text{tot}}} - \frac{C_2}{X_{\text{tot}}} - \frac{C}{X_{\text{tot}}} \right) - (d_1 + k_1) C_1 \right], \end{aligned} \tag{6.39}$$

in which the term in the square brackets is the retroactivity to the input r of the insulation device. The model of the insulation device with the downstream system remains the same as before and given by equations (6.26)–(6.29).

Figure 6.21 shows the trajectories of $Z(t)$, and $X^*(t)$ for the system of Figure 6.19. As desired, the signal $X^*(t)$, which drives the downstream system, closely tracks $A(t)$ plotted in Figure 6.20 despite the retroactivity due to load applied by the downstream sites p'. Note that because of a nonzero retroactivity to the input r of the insulation device, the trajectory of $Z(t)$ is slightly different from the same

trajectory in the absence of the insulation device (Figure 6.21a). The retroactivity to the output s only slightly affects the output of the insulation device (Figure 6.21b). The plot of Figure 6.21b, showing the signal that drives the downstream system, can be directly compared to the signal that would drive the downstream system in the case in which the insulation device would not be used (Figure 6.20, dashed red plot). In the latter case, the downstream system would not be properly driven, while with the insulation device it is even in the face of a large load.

Exercises

6.1 Include in the study of retroactivity in transcriptional systems the mRNA dynamics and demonstrate how/whether the results change. Specifically, consider the following model of a connected transcriptional system

$$\begin{aligned}\frac{dm_X}{dt} &= k(t) - \delta m_X,\\ \frac{dX}{dt} &= \kappa m_X - \gamma X + [k_{\text{off}}C - k_{\text{on}}(p_{\text{tot}} - C)X],\\ \frac{dC}{dt} &= -k_{\text{off}}C + k_{\text{on}}(p_{\text{tot}} - C)X.\end{aligned}$$

6.2 Consider the connected transcriptional system model in standard singular perturbation form with $\epsilon \ll 1$:

$$\frac{dz}{dt} = k(t) - \gamma(z - C), \qquad \epsilon\frac{dC}{dt} = -\gamma C + \frac{\gamma}{k_d}(p_{\text{tot}} - C)(z - C).$$

Demonstrate that the slow manifold is locally asymptotically stable.

6.3 The characterization of retroactivity effects in a transcriptional module was based on the following model of the interconnection:

$$\begin{aligned}\frac{dX}{dt} &= k(t) - \gamma X + [k_{\text{off}}C - k_{\text{on}}(p_{\text{tot}} - C)X],\\ \frac{dC}{dt} &= -k_{\text{off}}C + k_{\text{on}}(p_{\text{tot}} - C)X,\end{aligned}$$

in which the dilution of the complex C was neglected. This is often a fair assumption, but depending on the experimental conditions, a more appropriate model may include dilution for the complex C. In this case, the model modifies to

$$\begin{aligned}\frac{dX}{dt} &= k(t) - (\mu + \bar{\gamma})X + [k_{\text{off}}C - k_{\text{on}}(p_{\text{tot}} - C)X],\\ \frac{dC}{dt} &= -k_{\text{off}}C + k_{\text{on}}(p_{\text{tot}} - C)X - \mu C,\end{aligned}$$

in which μ represents decay due to dilution and $\bar{\gamma}$ represents protein degradation. Employ singular perturbation to determine the reduced X dynamics and the effects of retroactivity in this case. Is the steady state characteristic of the transcription module affected by retroactivity? Determine the extent of this effect as μ/γ decreases.

6.4 In this problem, we study the frequency dependent effects of retroactivity in gene circuits through simulation to validate the findings obtained through linearization in Section 6.3. In particular, consider the model of a connected transcriptional component (6.3). Consider the parameters provided in Figure 6.5 and simulate the system with input $k(t) = \gamma(1 + sin(\omega t))$ with $\omega = 0.005$. Then, decrease and increase the frequency progressively and make a frequency/amplitude plot for both connected and isolated systems. Increase γ and redo the frequency/amplitude plot. Comment on the retroactivity effects that you observe.

6.5 Consider the negatively autoregulated gene illustrated in Section 5.2. Instead of modeling negative autoregulation using the Hill function, explicitly model the binding of A with its own promoter. In this case, the formed complex C will be transcriptionally inactive (see Section 2.3). Explore through simulation how the response of the system without negative regulation compares to that with negative regulation when the copy number of the A gene is increased and the unrepressed expression rate β is decreased.

6.6 We have illustrated that the expression of the point of half-maximal induction in a covalent modification cycle is affected by the effective load λ as follows:

$$y_{50} = \frac{\bar{K}_1 + 0.5}{\bar{K}_2(1+\lambda) + 0.5}.$$

Study the behavior of this quantity when the effective load λ is changed.

6.7 Show how equation (6.9) is derived in Section 6.4.

6.8 Demonstrate through a mathematical proof that in the following system

$$\frac{dX}{dt} = G\,(k(t) - KX)\,(1 - d(t)),$$

in which $0 < d(t) < 1$ and $|\dot{k}(t)|$ is bounded, we have that $X(t) - k(t)/K$ becomes smaller as G is increased.

6.9 Consider the one-step reaction model of the phosphorylation cycle with downstream binding sites given in (6.20). Simulate the system and determine how the behavior of the connected system compares to that of the isolated system when the amounts of substrate and phosphatase X_{tot} and Y_{tot} are increased.

6.10 Demonstrate that the Jacobian $\partial f_1(x,u)/\partial x$ for the system in equations (6.30) has eigenvalues with negative real part. You can demonstrate this by using symbolic computation, or you can use the parameter values of Figure 6.16.

6.11 Demonstrate that the Jacobian $\partial f_1(x,u)/\partial x$ for the system in equations (6.37) has eigenvalues with negative real part. You can demonstrate this by using symbolic computation, or you can use the parameter values of Figure 6.18.

6.12 Consider the activator-repressor clock described in Section 5.5 and take the parameter values of Figure 5.9 that result in a limit cycle. Then, assume that the activator A connects to another transcription circuit through the reversible binding of n copies of A with operator sites p to form the complex C:

$$\mathrm{nA} + \mathrm{p} \underset{k_{\mathrm{off}}}{\overset{k_{\mathrm{on}}}{\rightleftharpoons}} \mathrm{C}$$

with conservation law $p + C = p_{\mathrm{tot}}$ (connected clock). Answer the following questions:

(a) Simulate the connected clock and vary the total amount of p, that is, p_{tot}. Explore how this affects the behavior of the clock.

(b) Give a mathematical explanation of the phenomenon you saw in (a). To do so, use singular perturbation to approximate the dynamics of the clock with downstream binding on the slow manifold (here, $k_{\mathrm{off}} \gg \gamma_A, \gamma_B$).

(c) Assume now that A does not bind to sites p, while the repressor B does. Take the parameter values of Figure 5.9 that result in a stable equilibrium. Explore how increasing p_{tot} affects the clock trajectories.

6.13 Consider the system depicted in Figure 6.19 and model the activator-repressor clock including the mRNA dynamics as shown in Section 5.5. Demonstrate through simulation that the same results obtained in Section 6.6 with a two-dimensional model of the clock still hold.